



Materials Horizons

Bulk Network Polymers with Dynamic B–O Bonds: Healable and Reprocessable Materials

Journal:	<i>Materials Horizons</i>
Manuscript ID	MH-REV-08-2019-001223.R2
Article Type:	Review Article
Date Submitted by the Author:	17-Oct-2019
Complete List of Authors:	Bapat, Abhijeet; Deakin University - Geelong Campus at Waurm Ponds, Institute for Frontier Materials Sumerlin, Brent; University of Florida, Department of Chemistry; Sutti, Alessandra; Deakin University - Geelong Campus at Waurm Ponds, Institute for Frontier Materials

SCHOLARONE™
Manuscripts

ARTICLE

Bulk Network Polymers with Dynamic B—O bonds: Healable and Reprocessable Materials

Abhijeet P. Bapat,*^a Brent S. Sumerlin*^b and Alessandra Sutti*^aReceived 00th January 20xx,
Accepted 00th January 20xx

DOI: 10.1039/x0xx00000x

The need to minimize the amount of polymeric waste entering landfills and oceans has led to several research avenues in the field of polymer science. Particularly, the development of intrinsically self-healing and reprocessable thermoset polymers containing dynamic crosslinks has garnered significant interest in the recent years. Reversible B—O bonds in certain organoboron compounds have shown great versatility and promise as dynamic crosslinks for the design of self-healing and reprocessable bulk polymer networks. This review provides an overview of the chemistry of organoboron species with dynamic B—O bonds amenable to the design of healable/reprocessable thermosets. Recent developments in this fairly young and interesting research topic are highlighted, along with a critical commentary on the scope and future challenges in designing robust dynamic materials with reversible B—O bonds.

Introduction

The use of synthetic polymers has been steeply rising since the end of World War II, and polymers have now infiltrated almost every imaginable aspect of human life. The popularity of synthetic polymers arises from their desirable material properties like low density, excellent durability, and a wide scope for tuning mechanical properties. However, the excellent durability and chemical inertness of commodity plastics also pose major concerns owing to their persistence in the environment for centuries, in the form of landfill and oceanic pollution.¹ Multiple research avenues towards making synthetic polymers more sustainable and reducing their environmental impact are being explored globally.² These include a) the use of renewable monomers³ b) the development of polymers that are degradable or amenable to depolymerisation for monomer recovery⁴ c) the development of healable or re-mouldable thermosets,^{5–7} and d) the development of new catalysts that facilitate polymerization, depolymerisation, or reprocessability.^{8,9}

Designing polymers that can undergo damage repair under suitable conditions is an attractive and logical way to prolong their service life and reduce their environmental impact by reducing the frequency at which they require replacement. Mendable, or healable polymers have the ability to restore their structure and useful properties, ideally indefinitely, through intrinsic or extrinsic damage-repair mechanisms depending on their design, during their service life.¹⁰ The damage can be caused through direct mechanical impact, or in the form of

micro-cracks and delamination caused by long term environmental exposure, chemical fumes, heat, etc.¹¹ Extrinsic healing involves the damage-induced release of polymerizable healing agents encapsulated within micro-reservoirs dispersed in the polymer, followed by their rapid flow and polymerization at the damage site. However, the depletion of healing agents at the repair site prevents multiple instances of damage repair at the same location. Intrinsic healing, on the other hand, relies on the reversible cleavage and re-formation of supramolecular or covalent bonds between individual polymer chains, enabling repeated healing at the same site under suitable conditions.

A large body of research involving intrinsically healable polymers incorporating non-covalent and dynamic covalent bonds has been reported in the past few years. The ready reversibility of non-covalent bonds such as hydrogen bonding,^{12–15} van der Waals interactions,¹⁶ π - π interactions,¹⁷ metal-ligand coordination,¹⁸ electrostatic interactions,¹⁹ and host-guest interactions²⁰ has been used to design healable polymer networks. Dynamic covalent chemistry^{21–23} offers a repertoire of reversible covalent bonds with higher stability, compared to non-covalent bonds, while affording reversibility under specific conditions or stimuli. Several reports on healable polymers based on dynamic covalent chemistry, including cycloaddition reactions,^{24, 25} thiol-disulfide exchange and disulphide metathesis,^{26, 27} thiol-Michael exchange,²⁸ radical-exchange reactions,^{29–32} olefin metathesis,³³ and transesterification reactions,³⁴ have been published in the recent past. The interested readers are advised to refer to some excellent reviews on self-healing polymers, covering various aspects of the topic, including design principles, various chemistries, and characterization methods.^{7, 35–43}

Based on the same principles of bond reversibility that enable intrinsic healing in polymeric materials, dynamic covalent chemistry also enables the design of re-mouldable or

^a Institute for Frontier Materials, Deakin University, Waurn Ponds, Victoria 3216, Australia. E-mail; a.bapat@deakin.edu.au; alessandra.sutti@deakin.edu.au

^b George & Josephine Butler Polymer Research Laboratory, Center for Macromolecular Science & Engineering, Department of Chemistry, University of Florida, Gainesville, Florida 32611, United States. E-mail: sumerlin@chem.ufl.edu

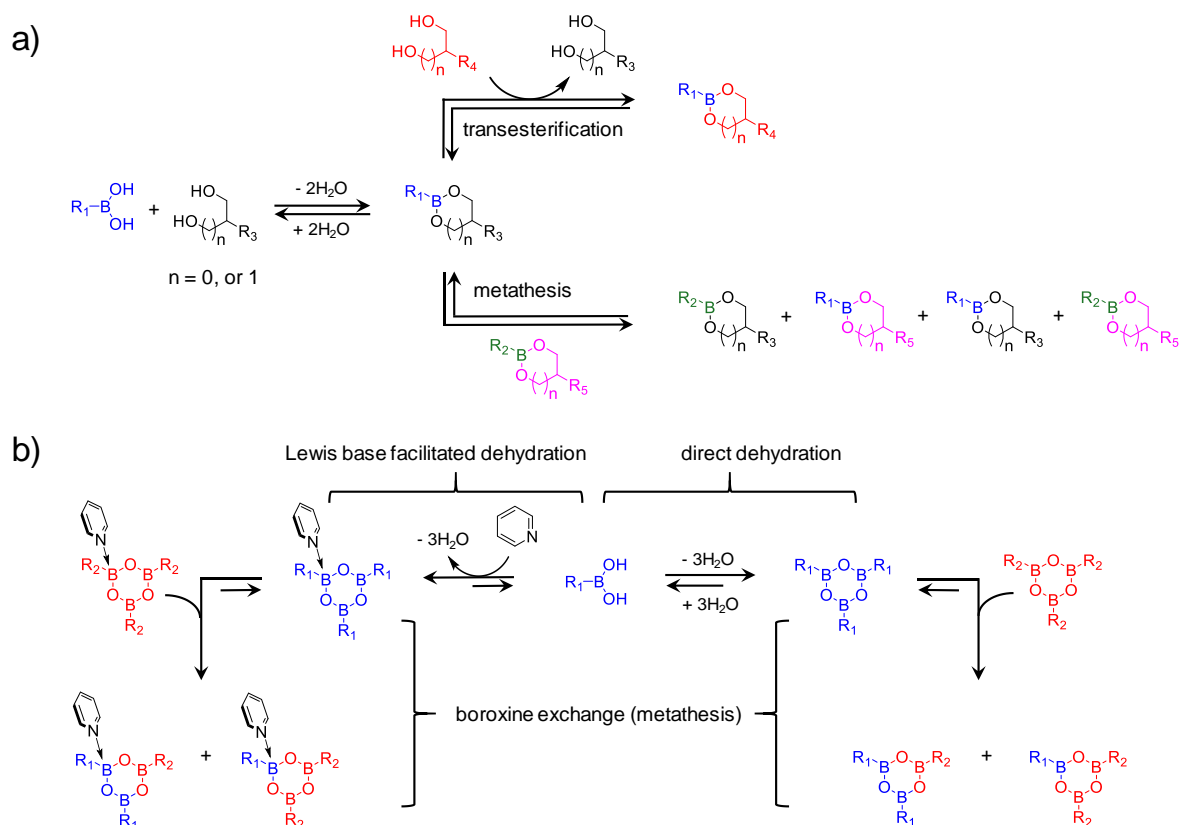
re-processable thermosets. Thermosets, or polymers with covalent crosslinks that percolate the whole mass, account for 15–20% of the global polymer production.^{44, 45} Their high mechanical strength, chemical stability, and processing costs often lower than thermoplastics, make them irreplaceable in a range of applications including adhesives, structural composites, electrical insulation, coatings, and others. However, unlike thermoplastics, conventional thermosets cannot be reprocessed due to their inability to melt and flow at high temperatures. In recent years, the incorporation of dynamic covalent bonds as exchangeable crosslinks within thermoset polymers has enabled their thermal reprocessability.^{45, 46} Such polymers, termed as “covalent adaptable networks” by Bowman and colleagues,^{47, 48} undergo bond exchange *via* two different mechanisms: dissociative and associative bond exchange. The dissociative mechanism of bond exchange is a two-step process which involves bond breakage, followed by bond reformation through reaction with complementary species at new sites (e.g., Diels-Alder reactions). During dissociative exchange, there is a reduction in crosslink density, allowing for topological rearrangements, followed by bond reformation. In the associative bond exchange mechanism, bond breakage and formation occur concurrently (e.g., metathesis and trans-esterification reactions), resulting in a constant crosslink density at all times. The covalent adaptable networks that operate *via* the associative exchange mechanism are also known as vitrimers due to their glass-like thermal reprocessability and flow behaviour, despite the constant crosslink density. Since the first report on vitrimers published by Leibler and co-workers⁴⁹ in 2011, various dynamic covalent exchange chemistries including transesterification reactions, transamination of vinylogous urethanes, transalkylation reactions of ammonium halide salts, siloxane-silanol exchange, olefin metathesis, and imine-amine exchange reactions have been successfully employed to design reprocessable thermosets.^{50–57}

Organoboron containing polymers manifest a number of interesting properties, owing to the tricoordinate, Lewis-acidic boron atom.⁵⁸ The electron deficient boron atom in organoboron polymers attains the desired octet configuration through overlap with π -donors, *via* Lewis acid-base pair formation, or coordination with nucleophiles, resulting in interesting photophysical, and catalytic properties. Boron-containing polymers have been used in diverse applications such as luminescent and optoelectronic materials,^{59–61} sensors,^{62–64} gel electrolytes for battery applications,⁶⁵ flame-retardants,⁶⁶ lubricant additives,⁶⁷ hydrogen donors for organic reductions,⁶⁸ and stimuli responsive materials for biomedical applications.^{69, 70} Jäkle and coworkers have recently utilized the Lewis pair formation between polymers containing pendent Lewis acidic organoboron groups and Lewis basic α,ω -pyridyl functional telechelic oligomers to design transient polymer networks.⁷¹ Arguably, from the perspective of this review, the hallmark of organoboron based polymers is the reversibility of the B—O bond in select organoboron species, making them highly useful reversible crosslinks in the design of dynamic polymer networks and gels. Notably, the reversible binding of

boronic acids^{72–80} and their cyclic analogues^{81–83} with 1,2- or 1,3-diols in aqueous media to yield tetrahedral boronate esters has been widely utilized for accessing stimuli responsive polymeric materials ranging from micellar nano-objects to hydrogels for a plethora of applications. We will exclude the discussion of organoboron based healable hydrogels (and organogels) in this review, and instead direct the interested readers to recent reviews on the topic.^{69, 84, 85} In contrast, the use of organoboron species with dynamic B—O bonds for the design of healable and/or reprocessable bulk polymeric materials has been reported only recently,⁸⁶ and has already garnered considerable research interest. The focus of this review paper is to provide an overview of the chemistry of organoboron species with dynamic B—O bonds amenable to the design of healable/reprocessable bulk polymer networks, and highlight the recent developments in this rapidly developing research area.

Boronic esters and boroxines are the two important organoboron species with dynamic B—O bonds amenable to the design of healable/reprocessable bulk polymers. Boronic esters are trigonal planar compounds reversibly formed through the binding of boronic acids and diols in the bulk or in anhydrous organic solvents. Boronic esters have lately been employed for designing degradable,⁸⁷ and architecture-transformable polymers.⁸⁸ The dynamic behaviour of the B—O bonds in trigonal planar boronic esters can be accessed in multiple ways — through hydrolysis/dehydration, through transesterification with externally added diols, and also via direct metathesis between different boronic ester compounds (Scheme 1a). The direct metathesis of boronic esters has been recently reported in the absence of detectable amounts of impurities or water, though additional investigation of the proposed mechanism could be warranted to eliminate the potential contribution of trace amounts of free diol or water.⁸⁹

The reversible dehydration of boronic acids to yield cyclic trimers called boroxines⁹⁰ (Scheme 1b), has also been used for designing dynamic polymer assemblies,^{91, 92} covalent organic frameworks,⁹³ and dynamic covalent libraries.⁹⁴ The boronic acid to boroxine equilibrium can be altered by the addition (or removal) of water. Lewis basic additives or substituents promote boroxine formation, likely through the reduction in the boron electrophilicity by imparting a partial sp^3 character to one or more boron atoms in the boroxine ring and sterically hindering the nucleophilic attack by water.⁹⁰ From the bulk polymer networks perspective, the Lewis-basic additives can also have a secondary role towards altering the network properties such as glass transition temperature and ductility.⁹⁵ The ability of different homo-substituted boroxine compounds to undergo direct exchange or metathesis reaction to afford hetero-substituted boroxines (Scheme 1b) has also been well established,^{94, 96} and recently utilized in healable networks and vitrimers with tunable mechanical properties.^{95, 97} It is important to note that while boronic ester formation requires two complementary functional groups (i.e., boronic acid, and diol), boroxines are obtained solely from the trimerization of boronic acids. This fundamental difference between boronic esters and boroxines affords different properties to the



Scheme 1 a) The reversible formation of boronic esters via the reaction of boronic acids with diols, their reversible transesterification with externally added diols, and their metathesis with externally added boronic esters, and b) the direct, and Lewis base facilitated reversible trimerization of boronic acids to boroxines, and the boroxine exchange (metathesis) reaction between two different boroxine compounds resulting in a mixture of homo, and hetero-substituted boroxines under equilibrium.

resulting dynamic polymers. For example, the crosslink density and mechanical strength of a boroxine linked network would be higher than that of a similar network bearing the same number of boronic ester links, due to the higher functionality of the boroxine. From a synthetic perspective, boroxine based networks are attractive since they can be obtained solely from boronic acid functional building blocks, compared to both boronic acid and diol functionality required for boronic ester based networks.

The following sections will highlight the research on healable and/or reprocessable bulk polymer networks based on both boronic esters and boroxines. For the convenience of the readers, the mechanical properties, healing, and reprocessing results for the various B—O bond based polymer networks discussed in the following sections have been summarized in Table 1.

Bulk networks based on boronic esters

Lavigne and co-workers⁸⁷ were the first to exploit the dynamic nature of trigonal planar boronic esters to prepare self-repairing linear polymers that could undergo reversible depolymerisation *via* hydrolytic cleavage of the boronic ester bonds in their main chain. Sumerlin and coworkers⁸⁶ reported the first 3D bulk polymer networks with dynamic boronic ester crosslinks that were capable of self-healing at room temperature. Low T_g polymer networks with varying crosslink densities were prepared via photoinitiated thiol-ene copolymerization of a boronic ester diene monomer with multifunctional thiols

(Figure 1a). When a disc-like sheet of the resulting polymer network was cut into two pieces and manually reconnected after wetting of the cut interface with water at room temperature, the material healed completely, resulting in near-complete disappearance of the scar (Figure 1b, and c). The sample could be stretched to more than twice the original length without fracture. Healing also occurred, albeit less efficiently, when the cut edges were joined without treatment with water, both under dry and humid conditions. Analogous to the hydrolysis of model small-molecule boronic esters, the small amount of externally added water enabled hydrolysis of the exposed boronic ester bonds at the cut surface to afford free boronic acid and diol, making them available for bond reformation with complementary species across the interface. The long time (3-4 days) required for near-complete healing at room temperature was attributed to the collective timescale required for healing *via* the generally accepted mechanism of chain diffusion across the cut interface, followed by bond reformation.⁹⁸ Near-complete recovery of tensile properties of the cut samples healed at 85% humidity for 3 days was observed for samples with varying crosslink densities (Figure 1d). While the samples with the highest crosslink density healed faster, repeated healing was demonstrated for up to 3 cycles for samples with the lowest crosslink density. Remarkably, crosslinked samples immersed in water for 60 days did not degrade, despite the vulnerability of the boronic ester crosslinks to hydrolysis. The overall hydrophobicity of the bulk material

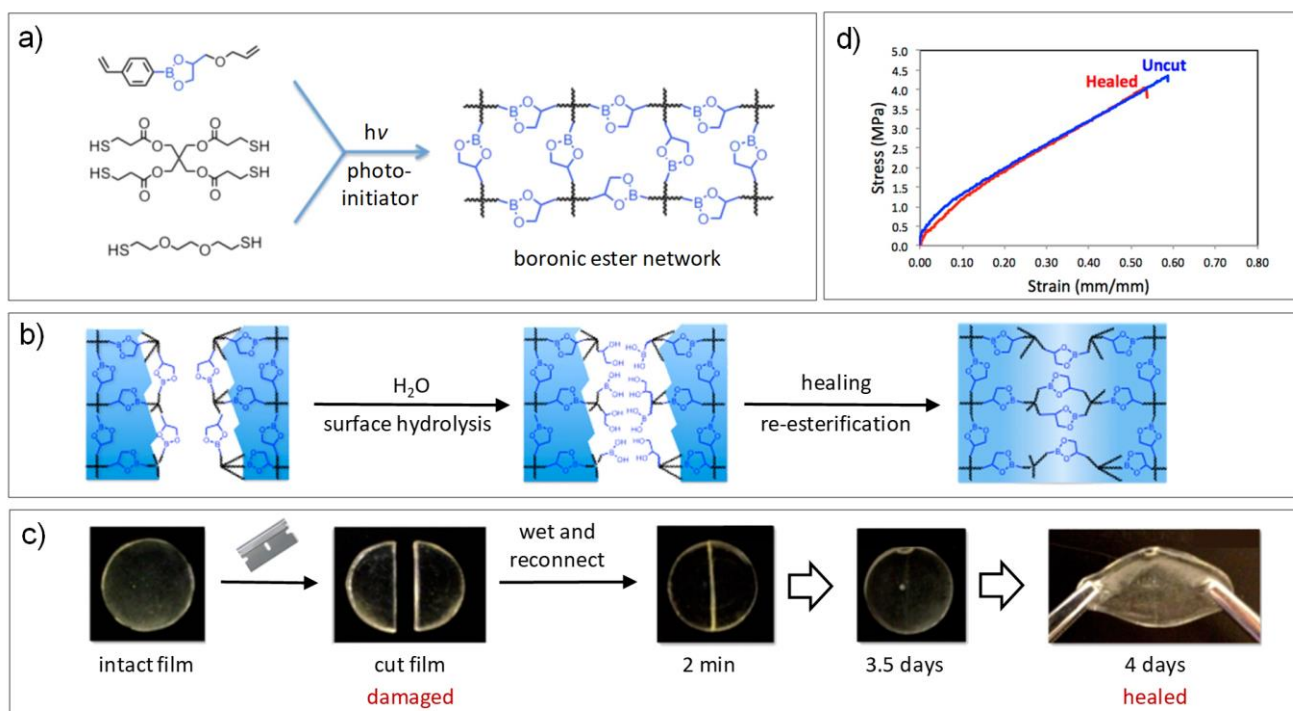


Figure 1 a) Synthesis of boronic ester networks *via* thiol-ene photochemistry b) Proposed mechanism of healing in polymer networks containing boronic ester crosslinks c) photographs of the healing process of a polymer network film containing boronic ester crosslinks d) tensile testing curves of the pristine and healed polymer networks indicating near-complete recovery of mechanical properties on healing. Reproduced with permission from ref. 86. Copyright 2015 American Chemical Society.

was sufficient to ensure hydrolytic stability of the boronic ester crosslinks spanning it.

A common drawback of incorporating fast exchanging dynamic bonds within bulk polymers is their propensity to undergo creep and stress relaxation at longer timescales.⁹⁹ The B—O bonds in the boronic esters within a dynamic polymer network can undergo exchange reactions *via* both dissociative, and associative mechanisms. In the dissociative exchange process, a boronic ester first undergoes hydrolytic cleavage to liberate the diol and boronic acid. The liberated reactive groups then undergo re-esterification with different complementary reaction partners to re-establish new crosslinks. In the associative exchange pathway, the boronic ester undergoes direct transesterification with another reactive group (e.g., free diol) present in excess, such that the average number of B—O bonds is maintained. Thus, depending on the mechanism, the exchange process in boronic esters can potentially occur at widely different time scales, making it an ideal dynamic bond for designing mechanically strong polymer networks that undergo reasonably fast healing.

Sumerlin and coworkers¹⁰⁰ also studied the isolated and combined effects of the incorporation of free diol functionality and/or permanent crosslinks into polymer networks containing dynamic boronic ester crosslinks on their healing efficiency and stress relaxation. Using thiol-ene photochemistry, they prepared three different subgroups of crosslinked polymers containing 1) various concentrations of free diol functionality to facilitate boronic ester exchange *via* both dissociative and associative pathways, 2) permanent crosslinks along with boronic esters to improve mechanical properties, and 3) both

free diol functionality and permanent crosslinks along with boronic esters (Figure 2a). All of the prepared network samples were hydrolytically stable when immersed in water for up to 13 days, although samples with higher amounts of free diol underwent noticeable creep and shape change.

Stress relaxation rates of network samples conditioned at different humidity levels (0%, 23%, and 85%) increased with increasing humidity and free diol functionality. The reduced influence of free diol content on stress relaxation at higher humidity levels also indicated that while transesterification (associative pathway) was the dominant mode of bond exchange in dry conditions (0%, and 23% humidity), bond exchange mostly happened through the hydrolysis and re-esterification (dissociative) pathway at 85% humidity. The significantly better healing demonstrated by networks containing free diol compared to those without free diol, under dry conditions, supported the conclusion that stress relaxation under dry conditions occurs through crosslink exchange by transesterification between the boronic esters and free diol.

As expected, network stress relaxation also decreased with an increasing ratio of permanent crosslinks to boronic ester crosslinks within the networks. In the absence of free diol functionality, the boronic ester networks having permanent crosslinks behaved like static networks, displaying minimal stress relaxation at low humidity levels, and moderate stress relaxation at high humidity levels. These results further reinforced the idea that network stress relaxation in the absence of free diol occurs mainly *via* the hydrolysis and re-esterification pathway. Samples containing up to 80% permanent crosslinks demonstrated near-complete recovery of

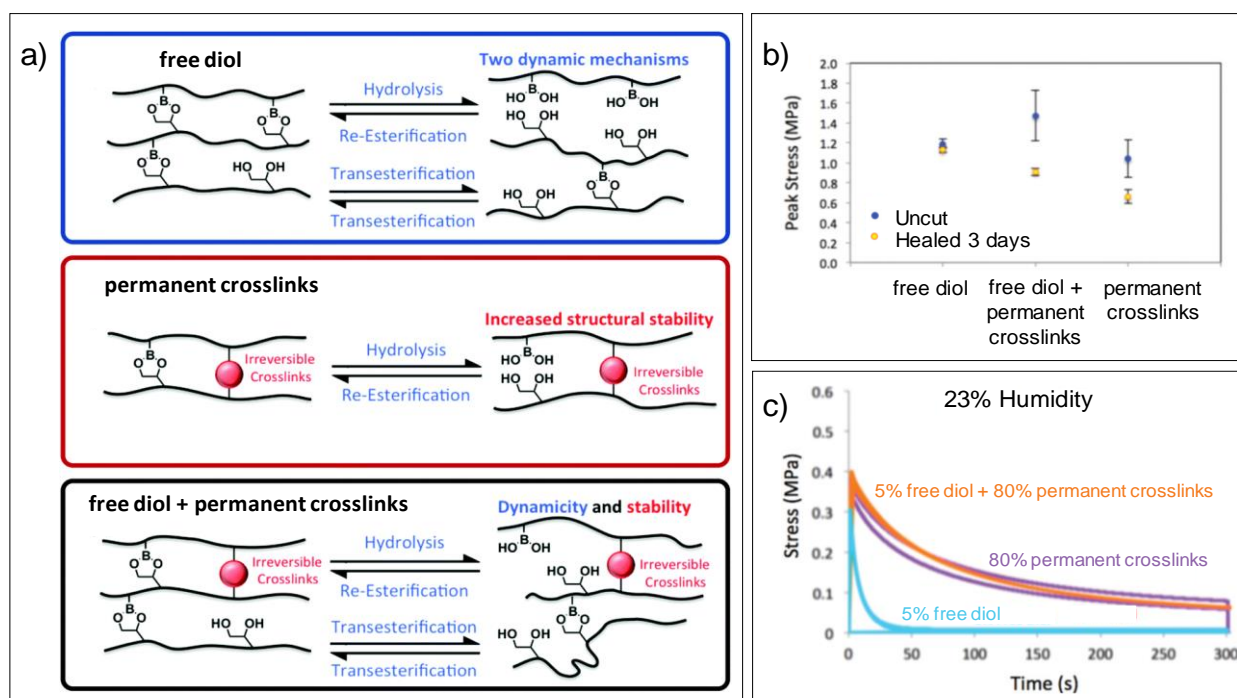


Figure 2 a) Representation of the boronic ester exchange pathways and the advantages of polymer networks containing free diol, or permanent crosslinkers, or both in synergy with dynamic boronic ester crosslinks b) Comparison of peak tensile stress values of pristine (blue dots) and healed (yellow dots) networks containing either free diol, or permanent crosslinks, or both along with dynamic boronic ester crosslinks c) Stress-relaxation curves of boronic ester crosslinked networks containing either free diol, or permanent crosslinks, or both at 23% humidity. Adapted with permission from ref. 100. Copyright 2018 Royal Society of Chemistry.

mechanical properties on healing at high humidity levels for up to 3 cycles.

Finally, the faster healing afforded by free diol functionality and the reduced stress relaxation and creep afforded by permanent crosslinks were combined, by inclusion of both these aspects within a single network containing boronic ester crosslinks. The stress relaxation behaviour of the resulting networks was similar to those containing permanent crosslinks alone. The healing efficiency of the hybrid networks was better than those containing permanent crosslinks, albeit lower than those containing only free diol.

Elastomeric systems have also been investigated following this path, with Zhang, Feng, and coworkers¹⁰¹ applying a similar approach to obtain silica nanofiller reinforced self-healing polymer composites. The crosslinked matrix was obtained *via* the thiol-ene photo crosslinking reaction between linear polydimethylsiloxane polymers bearing pendent thiol and vinyl groups, and a boronic ester-linked divinyl crosslinker. The vinyl functional polydimethylsiloxane polymers provided permanent crosslinks, while the boronic ester linked diol provided the dynamic crosslinks. However, the healing efficiencies of the resulting composite networks, as measured by tensile testing, were only 70% or lower.

Rubber-based matrices have also been investigated by Guo and coworkers¹⁰² who used the thermally initiated thiol-ene route for the crosslinking of commercially available styrene-butadiene rubber (SBR) with various amounts of a boronic ester-linked dithiol, to afford malleable and healable elastomer networks (Figure 3a). The mechanical properties of the resulting networks could be varied by tuning the amount of boronic ester crosslinker used. Similar to permanently crosslinked networks,

the Young's modulus and peak tensile strength of the rubbers increased with increasing crosslinker, accompanied by a decrease in elongation at break. The storage modulus and T_g of the networks also increased, indicating reduced chain mobility with increased crosslinking which is consistent with the higher amounts of added crosslinker. Notably, the associative (transesterification) bond exchange mechanism of boronic esters enabled the crosslinked networks to maintain their structural integrity at temperatures significantly higher than their T_g , as indicated by a constant value of storage modulus in the rubbery region. The dynamic B—O bonds also allowed for stress relaxation *via* network rearrangement at temperatures above T_g . Remarkably, stress relaxation was slower in networks with more boronic ester crosslinks, likely due to the retarded bond exchange owing to the restricted chain mobility at higher crosslink densities. Film samples of the crosslinked rubber, that were cut and rejoined manually, demonstrated efficient self-healing at 80 °C with >80% recovery of tensile properties after 24 h (Figure 3b). The healing efficiency initially increased with the amount of boronic-ester crosslinker, and peaked out at ~3 parts crosslinker per hundred parts of styrene-butadiene copolymer. This could be explained by the probability of B—O bond exchange increasing at higher boronic ester contents. However, the healing efficiency dropped, on further increasing the amount of crosslinker, suggesting a balancing interplay of improved bond exchange kinetics and the restricted chain mobility at higher B—O bond concentrations. The dynamic B—O bonds in the networks also enabled repeated reshaping and remoulding of samples at high temperature. The recycled samples had similar mechanical strength as the pristine samples, resulting in near-identical tensile curves (Figure 3c).

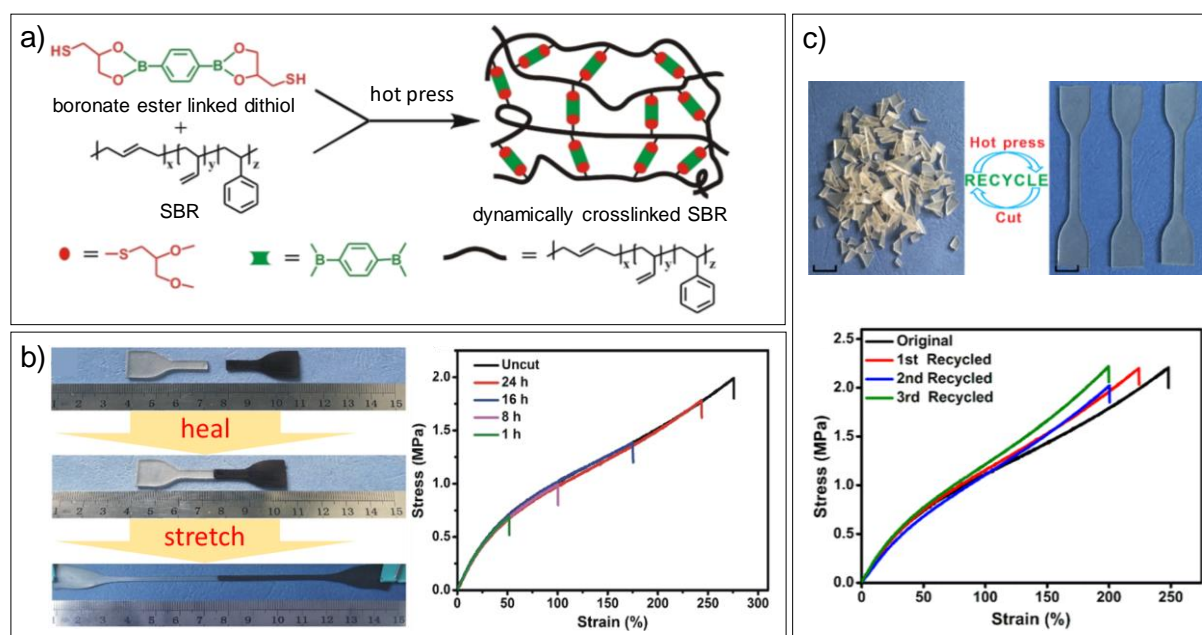


Figure 3 a) Crosslinking of styrene butadiene rubber (SBR) with boronic ester linked dithiol crosslinker *via* thermally initiated thiol-ene reaction b) Photographs showing cut and healed samples of SBR, and comparative stress-strain plots of pristine network and network samples healed for different durations at 80 °C c) Photographs showing the recycling process of the SBR network films, and the comparative stress-strain plots of original and recycled networks. Reproduced with permission from ref. 102. Copyright 2018 American Chemical Society.

Other interesting approaches have investigated the use of complementary mechanisms of dynamic crosslinking. Guo, Tang, and coworkers¹⁰³ demonstrated that combining dynamic covalent boronic ester crosslinks with weak and sacrificial Zn^{2+} -O coordination interactions within the same polymer network led to significant improvement in mechanical properties without any loss in the healing and reprocessing ability. A boronic ester dithiol was used to crosslink epoxidized natural rubber *via* the thiol-epoxide reaction, in presence of ZnCl_2 , to obtain networks with dynamic covalent boronic esters and a multitude of Zn^{2+} -O coordination interactions between zinc ions and pendent epoxide rings. Compared to networks with only boronic ester crosslinks, the networks with added ZnCl_2 exhibited increased modulus at room temperature, yet readily healed at 80°C, arguably due to the network rearrangement being facilitated by sacrificial dissociation of the noncovalent Zn^{2+} -O interactions. The materials also retained most of their mechanical performance after multiple recycling events. This work highlights the research potential in exploiting multiple types of dynamic bonds within the same networks to achieve healing and reprocessability without compromising the mechanical properties of thermosets for real world applications.

Leibler and coworkers⁸⁹ were the first to report the endothermic metathesis of boronic esters, wherein two different boronic ester molecules can directly and rapidly exchange their fragments under a mild thermal stimulus in the absence of detectable amounts of water or diol (Figure 4a and b). Using boronic ester metathesis as a means of B-O bond exchange, they prepared recyclable thermosets, called vitrimers due to their ability to flow like glass when heated. Polymers containing solely carbon-carbon bonds in the main chain and pendent boronic ester groups were obtained by two

complimentary approaches: 1) free radical copolymerization of boronic ester functional vinyl monomers, and 2) by a straightforward protocol for grafting boronic ester functional groups onto inert commodity plastics like polyethylene. Crosslinking of the polymer chains could be achieved *via* the thermally triggered cross metathesis with a difunctional boronic ester, either in solution or *via* reactive melt extrusion (Figure 4c). While the crosslinked polymers were no more soluble in good solvents for the uncrosslinked polymer chains, step-stress creep experiments proved they were able to flow like glass when heated (Figure 4d). Depending on the fraction of pendent boronic esters in the precursor polymers, the crosslinked networks had a low complex viscosity and could be extruded and moulded at temperatures typically employed for moulding commercial thermoplastics. Although the T_g of the vitrimers was slightly lower than the linear precursors, their mechanical properties were comparable. The elongation at break for the vitrimers was lower compared to the linear precursors, confirming successful crosslinking. Unlike their thermoplastic counterparts, the vitrimers exhibited improved melt strength and dimensional stability at high temperatures (Figure 4e) — features desirable for easy reprocessability and in-service damage repair of thermoset components. The vitrimers could be ground and reprocessed several times, confirming the robustness of the B-O bonds in boronic esters.

Remarkably, despite the vulnerability of the boronic esters to hydrolytic cleavage, the vitrimers performed exceptionally well in environmental stress-cracking and water uptake tests, compared to their thermoplastic counterparts. The versatility of boronic esters as dynamic linkages was further demonstrated by the thermal welding of vitrimers composed of conventionally incompatible polymers poly(methyl methacrylate) (PMMA), and high density polyethylene (HDPE). Specimens of PMMA and

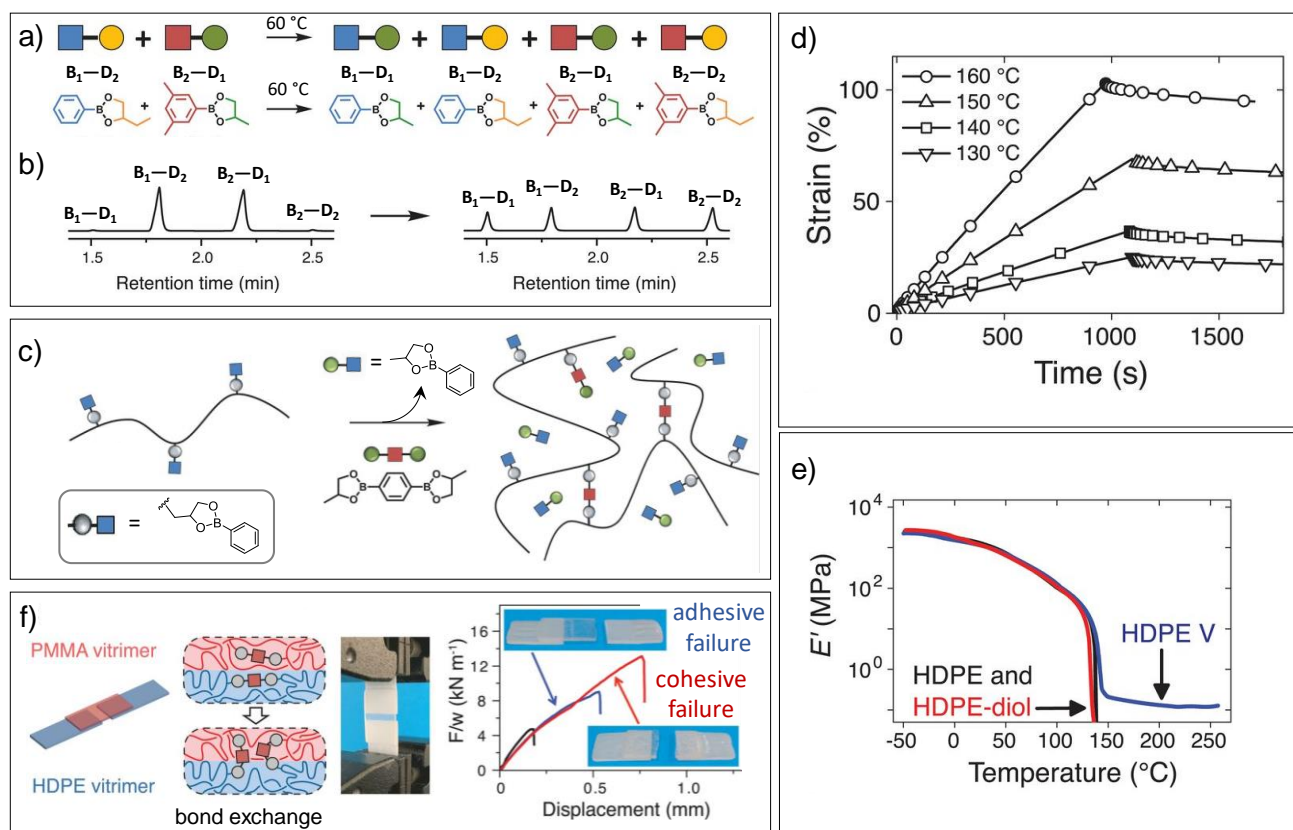


Figure 4 a) Schematic representation of thermally triggered direct metathesis between two model boronic esters to yield four different equilibrium products b) gas chromatographs of the metathesis reaction after 2 min (left), and 150 min (right) at 60 °C c) crosslinking of linear polymers with pendent boronic ester units via metathesis with a difunctional boronic ester crosslinker d) step-stress creep plots of a PMMA vitrimer showing the ability of the vitrimer to flow at high temperatures e) dynamic mechanical analysis curves of HDPE, HDPE-diol (with pendant diol units), and HDPE-V (HDPE vitrimer) showing improved melt strength of the vitrimer f) schematic representation, photo of the lap-shear testing process, and lap-shear results of the thermal welding of PMMA and HDPE vitrimer specimens via the boronic ester metathesis across the interface (black curve represents a negative control (contact time = 10 min, adhesive failure), while the blue curve (contact time = 10 min, adhesive failure) and the red curve (contact time = 20 min, cohesive failure) represent the PMMA/HDPE vitrimers. Adapted with permission from ref 89. Copyright 2017 AAAS.

HDPE, placed in contact under 11 kPa pressure and heated to 190 °C for 20 min, adhered so strongly that bulk PMMA failure (cohesive failure) occurred during lap shear testing (Figure 4f). The ability of the boronic ester links to undergo direct metathesis to form covalent bridges across the interface of the two chemically incompatible polymer surfaces makes them highly attractive in applications requiring joining and welding of components made of inherently incompatible polymers.

It is well known that the bulk viscoelastic properties of dynamic polymer networks largely depend on the kinetics of dynamics of the reversible crosslinks.¹⁰⁴⁻¹⁰⁷ The large effect of neighbouring groups on the equilibrium constants for boronic ester formation has been known for a long time.¹⁰⁸⁻¹¹⁰ Guan and coworkers¹¹¹ demonstrated that the neighbouring-group-assisted acceleration in the kinetics of boronic ester transesterification can be an effective tool for tuning the malleability and healing efficiency of bulk networks. They compared the transesterification rates of neopentyl glycol esters of phenylboronic acid, and its *o*-(dimethylaminomethyl) substituted variant, and found that the Lewis basic *o*-(dimethylaminomethyl) group increased the transesterification rate by almost 5 orders of magnitude (Figure 5a). The authors also synthesized two different difunctional boronic ester crosslinkers, mimicking the model compounds with disparate

transesterification kinetics (Figure 5b). Solutions of each of the two crosslinkers and a 1,2-diol functional linear polycyclooctene polymer were prepared in toluene. While the slow crosslinker (unsubstituted) led to gel formation in solution, the fast (*o*-(methylamino) substituted) crosslinker only led to a slight increase in viscosity of the polymer solution, qualitatively corroborating the effect of the different exchange kinetics of the two crosslinkers on macroscopic properties. Rheology studies indicated the crossover frequency (frequency above which the value of storage modulus G' exceeds the loss modulus G'') for the solution with the fast crosslinker was several orders of magnitude higher than that for the slow crosslinker — a manifestation of the influence of molecular properties on network dynamics. Stress-relaxation experiments performed on bulk polymer samples crosslinked with 1% of either crosslinker clearly showed the noticeably faster stress relaxation (increased malleability) afforded by the fast crosslinker (Figure 5c). Tensile testing of network films before and after being cut with a razor blade, re-joined manually and healed at 50 °C indicated almost quantitative healing in the networks with the fast crosslinker (Figure 5d). In contrast, the networks with the slow crosslinker showed poor or no healing. The results clearly confirmed the correlation between molecular-level dynamics and the macroscopic dynamics of the bulk polymers, thereby providing

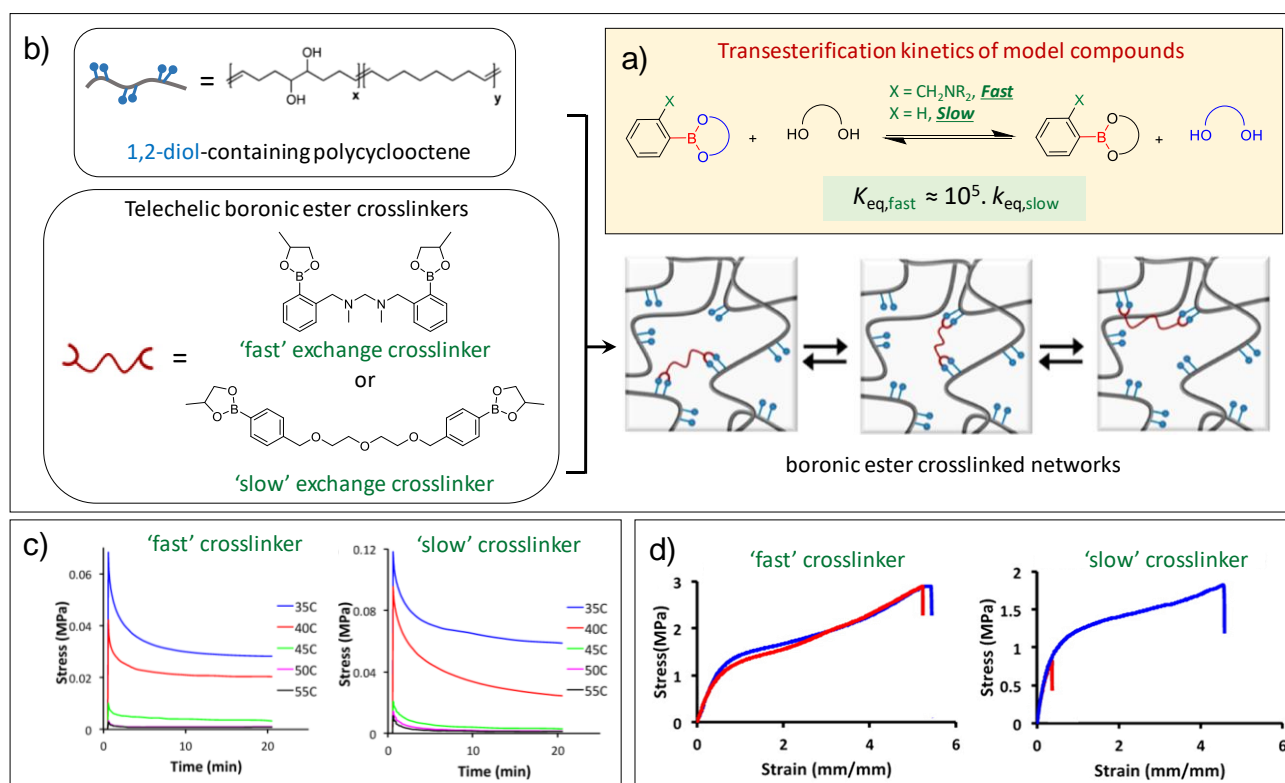


Figure 5 a) Kinetic studies on model compounds revealed that the *o*-(dimethylaminomethyl) substituted (fast) phenylboronic ester underwent transesterification at a rate almost 5 orders of magnitude faster than the unsubstituted (slow) phenylboronic ester b) Schematic representation of the synthesis of dynamic boronic ester networks via the transesterification reaction between a 1,2-diol containing polycyclooctene, and a 'fast' or 'slow' difunctional boronic ester crosslinker c) stress-relaxation plots showing the notably faster stress relaxation for the networks containing the 'fast' crosslinker at various temperatures d) tensile testing plots for the pristine (blue), and the healed (red) network specimens containing the 'fast' and the 'slow' crosslinker. Adapted with permission from ref 111. Copyright 2015 American Chemical Society.

useful cues for future design of dimensionally stable, yet rapidly healable polymers. The fast network dynamics afforded by the incorporation of the fast exchanging crosslinker also allowed for reprocessability. Network specimens could be cut into millimetre-size pieces and melt-pressed at 80 °C to the original shape for up to 3 cycles, with only a small deterioration in tensile properties. Further, the networks did not show any loss in mass or loss of mechanical strength on overnight immersion in water, indicating the local hydrophobic environment protected the boronic ester crosslinks from hydrolysis.

Yoshie and coworkers¹¹² reasoned that the higher hydrolytic stability of tetrahedral boronate esters (sp^3 hybridized boron), compared to trigonal planar boronic esters (sp^2 hybridized boron), made them more suitable as reversible crosslinks for moisture-assisted healing/reprocessing. The authors prepared bulk polymer networks with tetrahedral boronate esters having non-ionic B—N dative bonds as dynamic crosslinks. This was achieved by mixing a linear polymer bearing pendent catechol units (P(DA-co-BA)) with a para-dibenzeneboronic acid (PDBA) crosslinker and triethylamine (TEA) as the Lewis base for the formation of the B—N dative bonds with the Lewis acidic boron atom (Figure 6a). Solid state ¹¹B NMR spectroscopy confirmed the tetrahedral configuration of the boron atom in the boronate esters. Cyclic tensile testing under different humidity conditions revealed the increased malleability of the networks under high humidity conditions, owing to the moisture-induced reversibility of the tetrahedral boronate ester crosslinks.

Additionally, the temperature responsive B—N dative interactions also allowed for network rearrangement via thermally induced B—N bond cleavage and transesterification reactions, thus enabling the highly efficient moisture- or thermally-induced healing/reprocessability of the networks. For example, network samples with 60% PDBA crosslinker that were cut with a razor, re-joined manually, and maintained at 75% RH and 25 °C, showed complete recovery of tensile properties after 7 days (Figure 6b). The cut polymer films that were pressure reprocessed at 25°C after pre-conditioning at 75% RH, or under dry conditions at 60 °C, both showed complete recovery of mechanical properties as assessed by tensile testing (Figure 6c, and d). Notably, these networks also showed efficient healing under sea water, and less than 2% swelling on prolonged immersion in sea water, owing to the hydrolytic stability and ready reversibility of the tetrahedral boronate ester crosslinks.¹¹³

In the only report involving recyclable composites with dynamic B—O bonds, Jing and coworkers¹¹⁴ prepared fully recyclable carbon fibre-reinforced phenolic resin composite networks containing non-cyclic boronic esters as dynamic links. These composites possessed excellent mechanical properties and could be easily recycled via a mild alcoholysis process to obtain the clean fibre cloth and binder material. Composites obtained from the recycled cloth and binder had similar mechanical properties as the original composites.

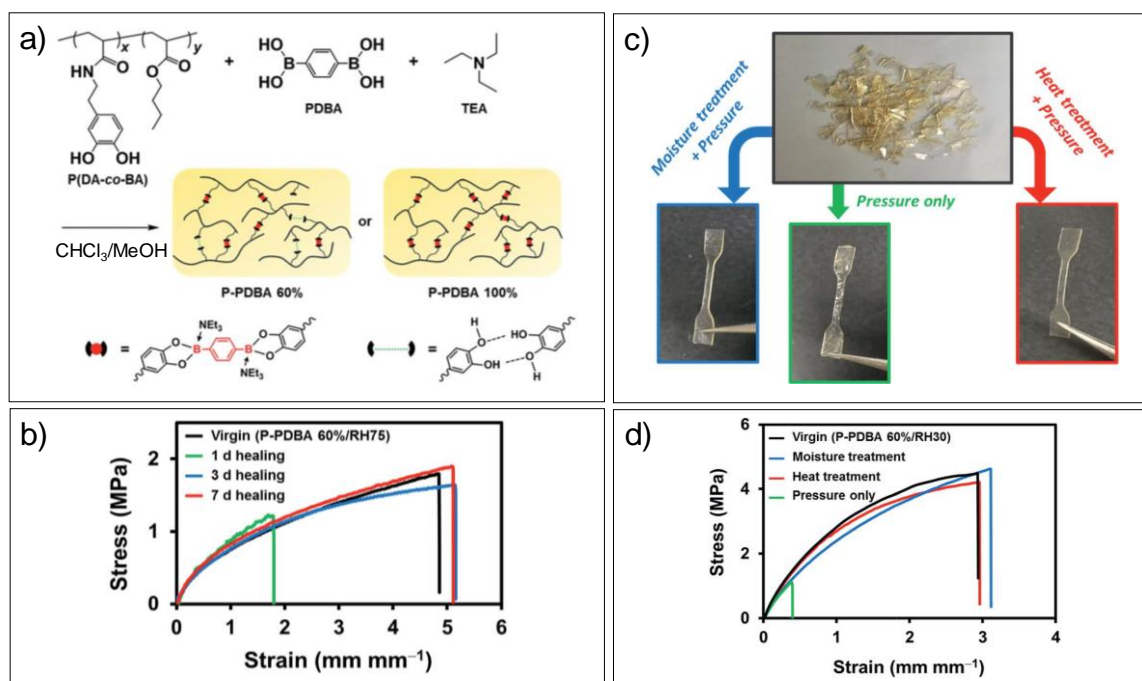


Figure 6 a) Schematic and cartoon representation of the synthesis of bulk networks containing tetrahedral boronate ester crosslinks with B—N dative bonds (and hydrogen bonds between excess catechol units) b) tensile testing plots showing complete recovery of mechanical properties for a network sample heated at 75% relative humidity and 25 °C for 7 days c) and d) High-pressure remoulded specimens, and tensile testing plots of the specimens obtained at 25 °C and 75% relative humidity, or at 60 °C under dry conditions demonstrating successful moisture- or heat-induced reprocessability (Note: the pressure only specimen was obtained at low humidity and 25 °C, as a negative control). Reproduced with permission from ref 112. Copyright 2018 Royal Society of Chemistry.

Boronic esters can form adducts with N-donor ligands through Lewis acid-base interactions. The strength of these supramolecular interactions depend on the electronic and steric contributions from both the reacting partners, as well as the solvent. In all the examples discussed above, the dynamic behaviour of the networks results from the dissociative or associative exchange of B—O bonds in the boronic ester junctions. However, it is important to highlight that several examples of supramolecular 2D and 3D networks where boronic ester junctions in polymeric (or macrocyclic) backbones serve as nodes for strand interconnection *via* dynamic B—N dative bonds with difunctional N-donor ligands have been reported.^{115–118} Severin and coworkers¹¹⁵ were the first to report the formation of such supramolecular networks by the multicomponent reaction between a trifunctional boronic acid monomer, a monofunctional catechol derivative, and a difunctional bipyridyl linker. Interestingly, control experiments where one of the three building blocks was excluded, did not result in network formation, suggesting that network formation occurred in two steps; the formation of the cyclic boronic esters, followed by crosslinking *via* B—N dative bond formation. The supramolecular networks could be reversibly disrupted or re-assembled on heating above 60 °C and cooling back to room temperature, owing to the thermoreversibility of the B—N dative bonds.

While B—N dative interactions have been used to accelerate exchange kinetics and improve the hydrolytic stability of dynamic B—O bonds in healable and reprocessable networks, the use of B—N dative bonds as complementary dynamic crosslinks in boronic ester based networks is so far unknown.

Inclusion of B—N dative crosslinks in conjunction with boronic esters (or boroxines) may help reduce creep and improve mechanical properties under normal usage conditions, while maintaining the fast B—O bond exchange essential for efficient healing and reprocessability at elevated temperatures.

Bulk networks based on boroxines

Bao, You, Li, and coworkers¹¹⁹ were the first to utilize boroxines as reversible crosslinks to access healable and reprocessable polymer networks. They synthesized stiff polymer networks that underwent water-assisted healing *via* hydrolytic dissociation of the boroxine crosslinks at the wet interface, followed by thermally assisted chain rearrangement and boroxine re-formation. Boronic acid end-functionalized linear telechelic poly(dimethylsiloxane) (PDMS) polymers were crosslinked *via* boroxine formation into a highly stiff polymer network that was able to support up to 450 times its own weight (Figure 7a). Tensile testing results revealed a very high Young's modulus (~180 MPa), and only about 10% strain at break indicating that the polymer was very stiff. However, stress-relaxation experiments suggested the network samples underwent very slow stress relaxation with time and the network chains likely had very poor segmental mobility to afford satisfactory self-healing ability. Surprisingly, when cut film pieces from two differently coloured network samples were wetted with water and joined manually at room temperature, the joined pieces could support their cumulative weight within several seconds. At 70 °C, slightly above the material's T_g (65 °C), complete recovery of peak stress and breaking strain values was observed within 12 h (Figure 7b). Thus, despite the limited chain mobility and high stiffness of the PDMS-boroxine networks, the application of water to the cut surfaces led to

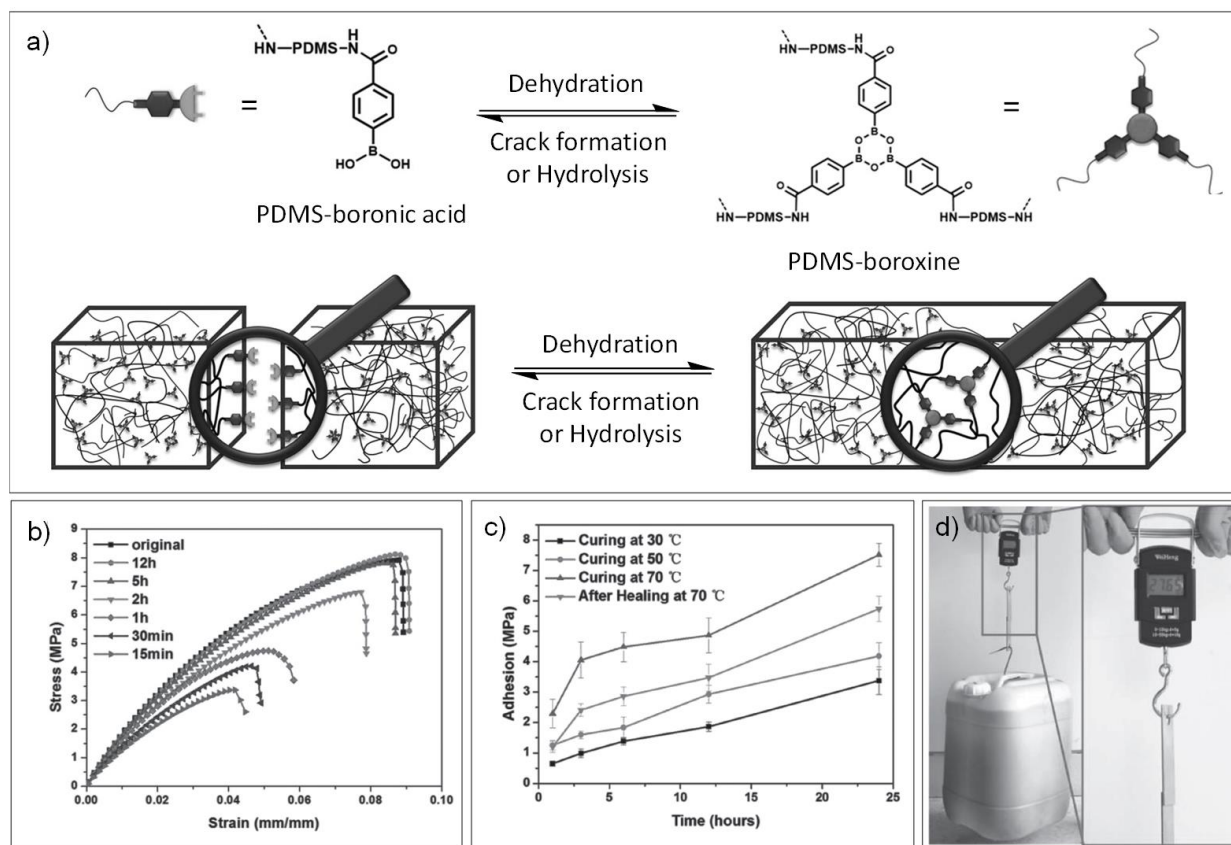


Figure 7 a) Structure of PDMS-boronic acid, and its reversible trimerization to form PDMS-Boroxine crosslinked healable 3D networks b) Stress-strain curves showing complete recovery of mechanical properties of the PDMS-boroxine networks that were cut, wetted with water, re-joined, and healed at 70 °C for 12 h c) Lap-shear adhesion strength results for steel specimens joined using the PDMS-Boroxine adhesive and cured at different temperatures, along with results for specimens healed at 70 °C after wetting and re-joining d) Image showing the steel specimens joined by the PDMS-boroxine adhesive can support a force of 27.65 kg (~271 N). Reproduced with permission from ref 119. Copyright 2016 John Wiley and Sons.

hydrolysis of the peripheral boroxines to boronic acids, enabling chain diffusion at the interface and efficient bridging *via* boroxine re-formation at 70 °C. The material also demonstrated repeated healing over many cycles, indicating the robustness of the boroxine crosslinks as dynamic linkages for damage repair. Lap-shear adhesion tests on steel specimens joined with the boroxine crosslinked PDMS at 70 °C, showed an adhesive strength of ~7.5 MPa, on par with commercial glues based on cyanoacrylates and epoxies (Figure 7c). The separated substrates could be re-joined by dipping the ends with the adhesive in water and curing at 70 °C for 24 h, albeit with a slightly lower adhesive strength (5.7 MPa). The bonded substrates could support a force of 27.65 kg (~271 N), proving the utility of PDMS-boroxine networks as strong, healable, and reusable adhesives for specialty applications. The bulk hydrophobicity of the PDMS-boroxine networks enabled them to maintain high stiffness (Young's modulus \approx 120 MPa) even after 3 days at 80% humidity.

Owing to the hydrolysable boroxine crosslinks, the PDMS-boroxine network films were able to soften at the surface on application of water and regained their hardness on drying. The authors utilized this soft-hard transition to coat a thin layer of silver nanowires onto water-softened PDMS-boroxine films to obtain semi-transparent, healable, conducting films. The strong bonding of the nanowires to the polymer was evident from the nearly constant resistivity of the film even after 100 cycles of adhesion and peeling test with a 3M scotch tape.

Analogous to the neighbouring group-facilitated acceleration of exchange kinetics in boronic esters discussed earlier, the ability of Lewis basic amino and pyridyl compounds to accelerate boroxine formation and stabilize the boroxine rings *via* coordination with the boron atoms is well known.^{90, 120} Sun, and coworkers¹²¹ prepared soft 3D networks *via* the trimerization of (o-aminomethyl) phenylboronic acid functional telechelic poly(propylene glycol) (PBA-PPG) oligomers (Figure 8a). Cut samples of the soft films from the resulting N-boroxine-PPG networks could undergo self-healing within 6 h, at room temperature. However, the resulting materials had poor mechanical properties (ultimate tensile strength = 0.19 MPa) due to the low glass transition temperature ($T_g = -55$ °C), to be useful for load-bearing applications. In order to improve the mechanical properties of the N-coordinated boroxine networks, poly(acrylic acid) (PAA) was blended at different mass ratios with the (PBA-PPG) oligomers before boroxine formation. The mechanical properties of the resulting N-boroxine-PPG/PAA composite networks could be tuned, based on the weight fraction of the PAA in the blend. The tensile strength (1.7 MPa to 12.7 MPa) and Young's modulus (2.7 MPa to 112 MPa) of the composite networks significantly increased on increasing the mass percent of PAA from 6 to 40, with a corresponding decrease in the tensile strain at break (661% to 81%) (Figure 8b). The authors attribute the significantly improved mechanical properties of the composites to the formation of an interpenetrating network through a combination of hydrogen-bonding interactions between secondary amine groups of PBA-

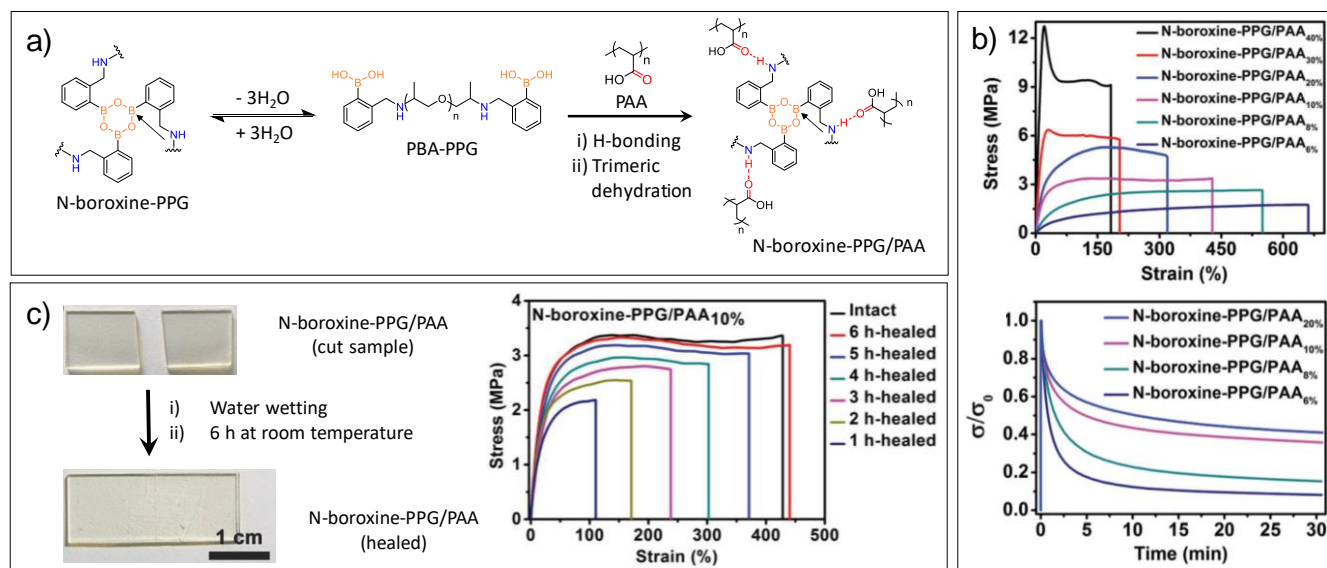


Figure 8 a) Synthetic pathways to self-healing N-Boroxine-poly(propylene glycol) (N-Boroxine-PPG) networks, and N-Boroxine-poly(propylene glycol)/poly(acrylic acid) (N-Boroxine-PPG/PAA) composites b) Stress-strain (top) and stress-relaxation (bottom) plots showing the increase in mechanical toughness and stress-relaxation time with increasing PAA content of the composites, and c) Images showing the self-healing of a cut, wetted, and manually re-joined specimen of N-Boroxine-PPG/PAA along with a stress-strain plot showing the restoration of mechanical properties within 6 h of healing. Adapted with permission from ref 121. Copyright 2018 John Wiley and Sons.

PPG and carboxylic acid groups of PAA, and the dynamic N-coordinated boroxine links joining the PPG chains. However, no evidence to rule out the formation of ionic bonds between the basic amine groups of PBA-PPG and the pendent carboxylic acid groups of PAA was provided. Notably, the hydrophilic PAA made the composites sensitive to changes in humidity, resulting in a deterioration in mechanical properties at high ambient humidity. Stress-relaxation studies of the N-boroxine-PPG/PAA composites revealed that the composites with higher PAA contents underwent slower stress-relaxation, likely due to the reduced number of dynamic boroxine links that are essential for stress-relaxation.

The N-boroxine-PPG/PAA composites underwent water assisted self-healing at room temperature to afford near-complete restoration of mechanical properties. The healing efficiency increased initially with increasing PAA content and was a maximum (99% healing in 6 h) at 10% PAA content (Figure 8c). However, the healing efficiency decreased with further increase in PAA content reaching only 87% after 18 h, for the composite with 40% PAA. The authors attribute the initial increase in healing efficiency with PAA content to the combined effect of boroxine and hydrogen bond reshuffling involved in the healing process. They inferred that further increase in the PAA content resulted in reduced chain mobility, leading to slower stress relaxation and incomplete healing at room temperature. Owing to the presence of dynamic boroxine, and hydrogen bonds, the N-boroxine-PPG/PAA composites could be readily reshaped and recycled under a mild pressure of 0.4 kPa at room temperature. Tensile testing confirmed the complete restoration of mechanical robustness even after repeated recycling for up to five cycles.

Dubois, Gerbaux, Raquez, and co-workers¹²² demonstrated that the boronic acid/boroxine equilibrium occurs even when the phenylboronic acid exists as an o-iminoboronate *via* a dative interaction of the boron with an N-donating imine substituent in the ortho position. Initially, they confirmed the reversible boroxine formation through dehydration of model o-iminoboronate compounds. Later they prepared 3D networks

through the dehydrative boroxine formation of telechelic α,ω -bis(o-iminoboronate)-poly(propylene glycol) (o-iminoboronate-PPG) oligomers (Figure 9a). The mechanical strength of the resulting networks depended on the crosslink density and ambient humidity. The boroxine networks prepared with α,ω -bis(o-iminoboronate)-PPG of average molecular weight ≈ 2000 g/mol resulted in a stretchy, rubbery material that turned into a highly viscous, syrupy liquid on exposure to ambient air at 35% humidity. On heating to 70 °C, boroxine re-formation occurred, restoring the initial rubbery properties of the networks. Boroxine networks prepared with α,ω -bis(o-iminoboronate)-PPG of average molecular weight ≈ 400 g/mol, were mechanically stronger, owing to the reduced chain length between crosslinks (Figure 9b). The higher crosslink density also helped in the conservation of mechanical properties even on exposure to ambient humidity (35% RH) for 48 h (Figure 9c), owing to the reduced susceptibility of the boroxines to hydrolysis. Tensile tests performed on specimens of the more-crosslinked networks before and after being manually cut with a razor blade, re-joined, and healed at room temperature and 35% relative humidity, indicated $\sim 93\%$ recovery of the strain at break, and $\sim 92\%$ recovery of Young's modulus (Figure 9d). Samples healed in dry environments did not undergo healing, indicating the important role of boroxine bond hydrolysis and re-formation (dissociative pathway) across the cut interface in the healing process.

While sufficient chain mobility, necessary for achieving satisfactory healing/remoulding, is often related to flexibility and malleability of matrices, excellent healing and reprocessability have also been observed in stiff networks. Dubois, Gerbaux, Raquez, and co-workers¹²³ reported the synthesis of highly stiff and healable non-isocyanate based polyurethane networks with dual dynamic iminoboronate and boroxine crosslinks. The combined contribution of the dynamic boroxine and iminoboronate bonds towards healing and recyclability was confirmed by comparison with control networks containing either boroxine or imine bonds alone. Despite the presence of abundant dynamic bonds, the resulting

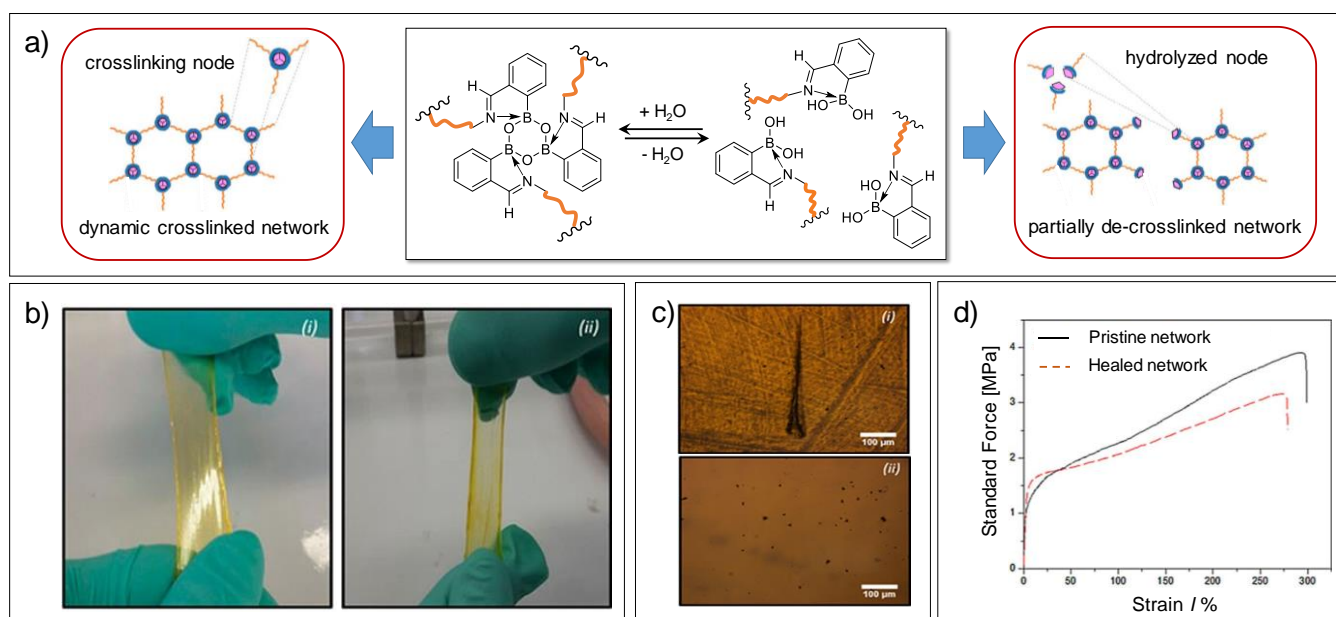


Figure 9 a) Schematic representation of the reversible dehydration of α,ω -bis(o-iminoboronate)-poly(propylene glycol) (α,ω -bis(o-iminoboronate)-PPG) to form dynamic boroxine crosslinked networks b) Network film obtained from α,ω -bis(o-iminoboronate)-PPG ($M_n, \text{avg} = 400 \text{ g/mol}$) oligomers i) before, and ii) after exposure to 35% relative humidity c) Scratched network film i) before, and ii) after healing for 48 h d) Tensile stress-strain curves of the pristine network (black), and the network after healing for 48 h (red), indicating ~93% recovery of the strain at break. Adapted with permission from ref 122. Copyright 2017 John Wiley and Sons.

networks were highly stiff (Young's Modulus = 551 MPa, and tensile strength = 11 MPa). Yet, these networks could be thermally healed and reprocessed for multiple cycles without loss of mechanical performance. The polymer networks also underwent efficient healing on exposure to 70% relative humidity at room temperature, owing to the hydrolysis and reformation of boroxine crosslinks. The highly stiff networks became malleable on exposure to 70% relative humidity at room temperature, owing to the reduced crosslink density resulting from the hydrolysis of some of the boroxine crosslinks. This enabled material reshaping just by exposure to high humidity at room temperature.

The boroxine based dynamic networks discussed so far exploit the dissociative bond exchange pathway involving the hydrolytic cleavage, and dehydrative re-assembly of boroxine crosslinks. While the possibility of accessing boroxine based dynamic polymers that heal *via* the associative pathway has been well supported by the existence of dynamic covalent libraries containing heteroarylboroxines obtained as an equilibrium product of a mixture of boronic acids,⁹⁴⁻⁹⁶ true vitrimers based on the boroxine exchange (or metathesis) have been only reported recently. Guan and coworkers⁹⁵ demonstrated using model compounds that similarly to the boronic ester metathesis, two different homo-boroxines can indeed undergo direct exchange or metathesis to yield hetero-substituted boroxines under thermodynamic equilibrium (Figure 10a). Inspired by these findings in low molecular weight model compounds, they utilized the boroxine exchange reaction as the associative bond-exchange pathway for designing strong and malleable thermosets that behave as true vitrimers. Initially, the kinetics of exchange reaction between model boroxine compounds was studied using ^1H NMR spectroscopy, and peak coalescence procedures were used to calculate 81.6 kJ/mol as the activation energy for the exchange reaction. Interestingly, while Lewis bases are known to facilitate boroxine formation, adding pyridine did not reduce the

activation energy of the exchange reaction. This observation led the authors to conclude that the boroxine exchange is facilitated by traces of free boronic acid resulting from hydrolysis due to extraneous moisture. Subsequently, a flexible diboronic acid monomer was synthesized and dehydrated in presence of either pyridine, or 4-undecylpyridine as the Lewis base to obtain 3D networks with ligand-bound boroxines as dynamic crosslinks (Figure 10b). Notably, pyridine containing networks were highly stiff and brittle, while, those containing 4-undecyl pyridine were ductile and tough, due to the plasticizing effect of the pendent undecyl groups (Figure 10c). As expected, the boroxine networks were insoluble in common organic solvents, but dissolved in methanol *via* methanolysis of the boroxines. By titration of the water formed through methanolysis, the extent of crosslinking was estimated to be almost 90%. Despite the highly crosslinked structure, and high toughness of the boroxine networks (Young's modulus = 560-770 MPa, tensile stress = 18-33 MPa, and elongation to break = 5-14%), they were highly malleable. Stress relaxation experiments, indicated that the material relaxed faster at higher temperatures, and a linear correlation existed between the log of relaxation time ($\ln(\tau)$) and the inverse of temperature ($1000/T$), implying the material possessed Arrhenius flow characteristics typical of a vitrimer (Figure 10d). Notably, the activation energy for network relaxation was in good agreement with that of the boroxine exchange reaction, responsible for network dynamics and malleability. Consequently, the polymer networks could be repeatedly reprocessed by hot pressing at strength, while affording fast network dynamics. The N—B dative coordination achieved through externally added amines also allows for tuning of the mechanical properties through the plasticizing or stiffening effect of the amine ligand. Building upon this work, Sun and coworkers⁹⁷ have recently demonstrated that by the careful tuning of the molar ratios of bifunctional and trifunctional

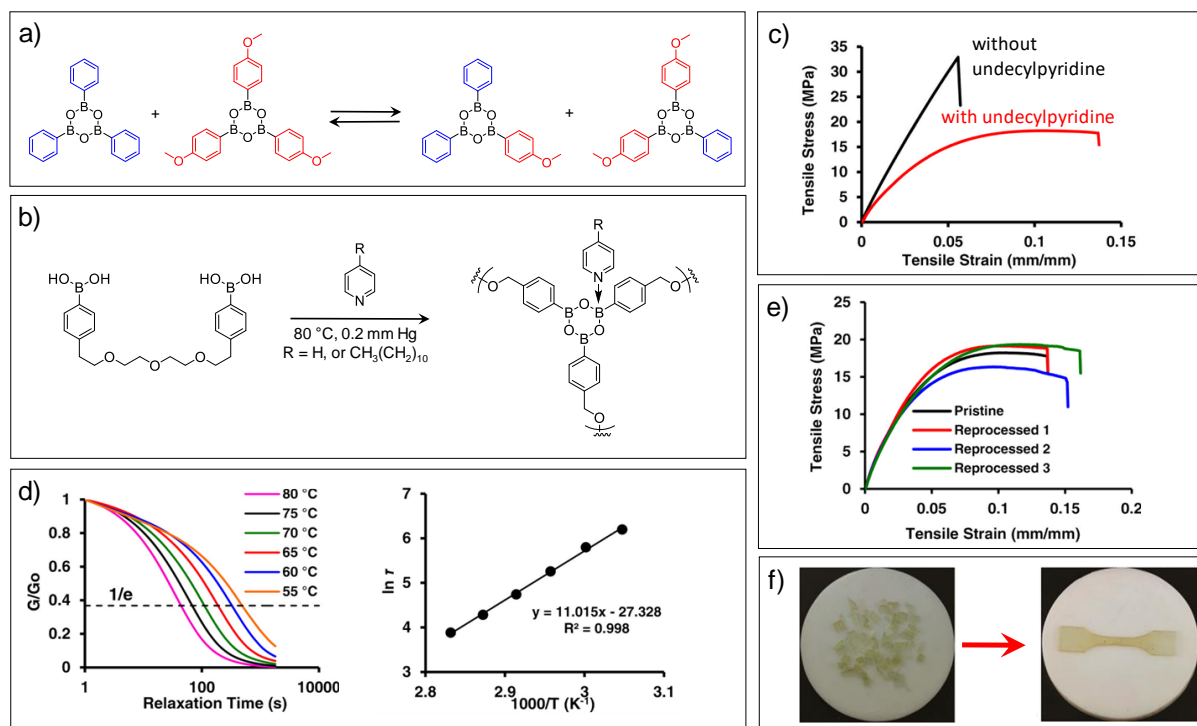


Figure 10 a) The boroxine exchange (metathesis) reaction between two model boroxine compounds b) Schematic for the Ligand-bound boroxine network synthesis c) Stress-strain curves for the boroxine networks with and without undecylpyridine d) Stress relaxation tests at various temperatures (left), and the Arrhenius plot with linear fit (right), confirming the true vitrimer-like behaviour of the undecylpyridine-bound boroxine networks e) Stress-strain curves for the pristine and hot-press reprocessed undecylpyridine-bound boroxine networks f) images of the cut pieces of the undecylpyridine-bound boroxine thermoset before, and after hot pressing. Adapted with permission from ref 95. Copyright 2018 American Chemical Society.

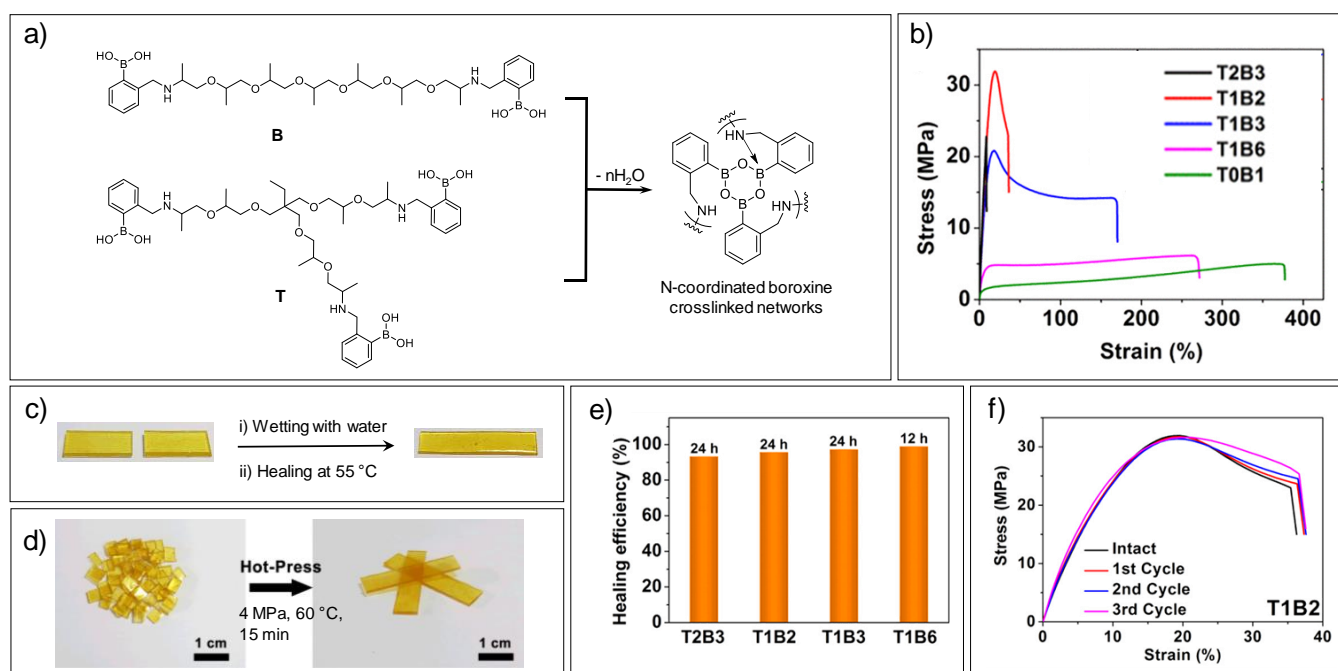


Figure 11 a) Schematic representation of the synthesis of N-coordinated boroxine crosslinked networks from bifunctional (B) and trifunctional (T) boronic acid monomers b) Tensile stress-strain curves of boroxine networks prepared from various ratios of T and B monomers (each number in the notations represents the moles of the monomer preceding it; for e.g., T1B2 indicates that the molar ratio of T to B in that polymer is 1:2) c) Images of a polymer film before and after healing d) Images showing cut pieces of boroxine based thermoset polymer films after thermal remoulding into the shape of the original films e) a column chart indicating excellent healing efficiency demonstrated by polymers prepared in varying ratios of B and T f) Representative tensile stress-strain curves confirming the complete recovery of mechanical strength of the polymer T1B2 for up to 3 reprocessing cycles. Adapted with permission from ref 97. Copyright 2019 American Chemical Society.

boronic acid building blocks, the crosslink density and mechanical properties of the resulting boroxine networks can be tailored between soft-and-tough to stiff-and-tough. Nitrogen coordinated boroxine networks were obtained

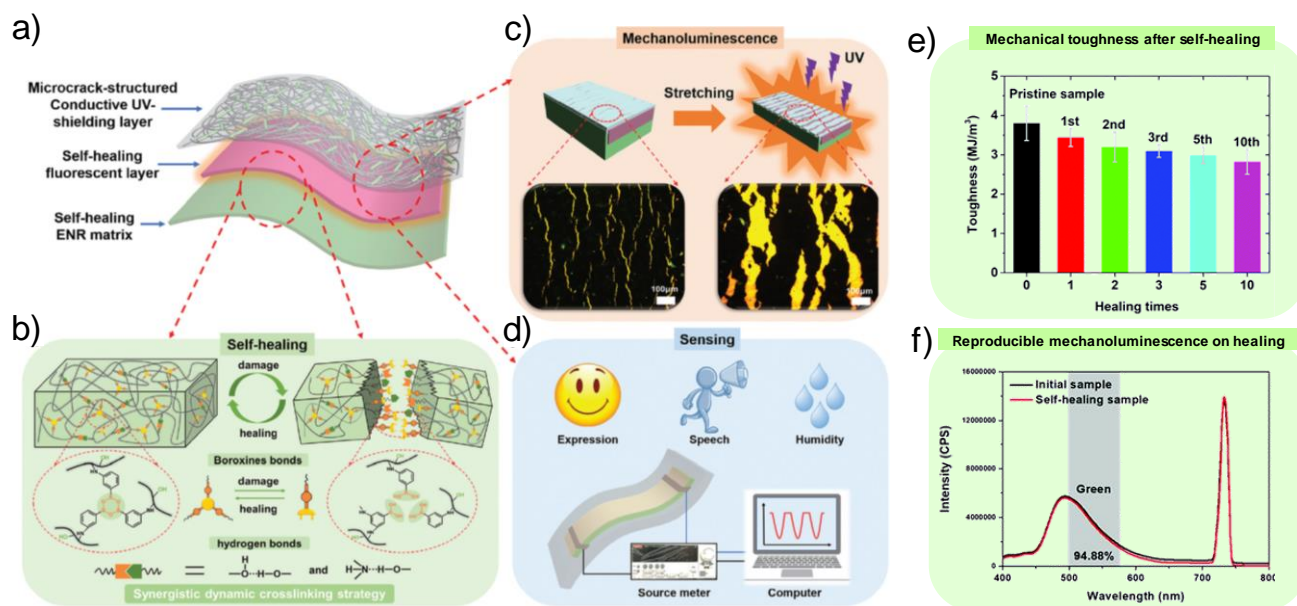


Figure 12 a) Compositional schematic of the 3-layered multifunctional composite material with luminescence, self-healing and sensing abilities (b) representation of the synergistic dynamic crosslinking network design comprising boroxines and hydrogen bonds for efficient and repeated self-healing (c) mechanoluminescence of composite materials due to the formation and reversible widening of microcracks in the top UV-shielding CNC/ CNT layer (d) cartoon representation of the composite material's ability to detect both human motion and humidity variation, owing to the changes in the resistance of the conductive CNC/CNT layer in response to strain and humidity (e) Column chart showing excellent recovery of mechanical toughness of the composite even after 10 healing cycles (f) 1D fluorescence spectra of a green fluorescent composite, before and after healing, indicating near-complete conservation of fluorescence upon healing. Adapted with permission from ref 124. Copyright 2019 Royal Society of Chemistry.

through the co-condensation of the bifunctional (B), and trifunctional (T) ortho-aminomethyl substituted boronic acid monomers (Figure 11a). While the networks obtained entirely from B were soft, yet tough (tensile stress ≈ 6 MPa, Young's Modulus ≈ 64 MPa, and elongation at break $\approx 375\%$), those obtained exclusively from T were too brittle to be characterized by tensile tests owing to their extremely high crosslink density (Figure 11b). An optimized network obtained *via* the co-condensation of B and T in the molar ratio of 3:2 (denoted as T2B3) was the strongest of all combinations that could be characterized by tensile testing (tensile stress ≈ 23 MPa, Young's Modulus ≈ 330 MPa, and elongation at break $\approx 23\%$). Owing to the high reversibility of the nitrogen-coordinated boroxine crosslinks, cut pieces of the network polymers underwent efficient healing after exposure of the cut edges to water (to facilitate boroxine hydrolysis) for one minute, re-joining the pieces, and heating at 55 °C for 24 h (to facilitate chain rearrangement and boroxine re-formation) (Figures 11c, and e). The polymer networks, although strong, could also be readily recycled under mild conditions, owing to the thermally triggered direct metathesis of nitrogen-coordinated boroxine crosslinks. Tiny pieces cut from the polymer sheets were collected in a Teflon mould and remoulded by hot pressing under a pressure of 4 MPa at 60 °C for 15 min (Figure 11d). Tensile testing curves of the recycled polymers were identical to those of the pristine polymer network, indicating complete recovery of mechanical properties on recycling (Figure 11f).

Self-healing polymeric materials are not only expected to regain their mechanical strength on healing, but also other properties essential for the utility of components made from them. Zhang and coworkers¹²⁴ utilized a combination of boroxines and hydrogen bonds as dynamic links in a modified (epoxidized) natural rubber (ENR) based matrix to design a multilayered cephalopod skin mimicking material with

mechanoluminescence, self-healing, and sensing abilities. The 3-layered material had a thick self-healing rubber film as the base layer, with a thin film of the healable rubber with fluorescent additives as the middle layer, and a mixture of cellulose nanocrystals (CNCs) and carbon nanotubes (CNTs) as the UV-shielding and conductive top layer (Figure 12a). The multilayered films showed no fluorescence in the unstretched state due to complete UV-shielding by the top CNC/CNT layer. However, on stretching the film, the top CNC/CNT layer developed micro cracks perpendicular to the stretching direction, allowing UV light to illuminate the underlying fluorescent layer resulting in strain-dependent mechanoluminescence (Figure 12c). Owing to the synergistic effect of the dynamic boroxine and hydrogen bonds as crosslinks in the rubber matrix (Figure 12b), the multi-layered films demonstrated excellent room temperature healing with 91%, and 74% recovery of toughness after the first, and the tenth healing cycles, respectively (Figure 12e). Moreover, the healed films display fluorescent spectra nearly identical to that of the pristine films (Figure 12f). Even after 10 cutting/healing cycles, the fluorescent healing efficiency was $\sim 81\%$. Due to the strain-, and humidity-dependent change in the electrical conductivity of the top UV-shielding layer, the composite films could be used as human motion sensors for decoding facial expressions and speech, and also as humidity sensors (Figure 12d). Notably, the sensing response of the healed films to motion and humidity was identical to that of the pristine films, indicating the excellent durability and sensing ability of the composite films.

Scope, opportunities, and open challenges

Dynamic polymeric materials can be designed to manifest tailored properties through a careful choice of building blocks that influence both dynamic, and static behaviour. The physical,

chemical, and functional properties under normal usage conditions (*i.e.*, static properties) are dictated by the choice of structural components that influence the network architecture, polymer morphology, and material properties.¹²⁵ On the other hand, the dynamic behaviour depends on the type, number, distribution, and the synergy between different types of reversible bonds embedded as network junctions. The presence of permanent crosslinks within a dynamic network also confers shape-memory and can serve to reduce creep within dynamic networks. Such a large number of design variables leads to near-infinite possibilities in terms of potential applications, ranging from healable soft devices,¹²⁶ to reprocessable/repairable high strength polymer composites.¹²⁷

The purpose of incorporation of dynamic crosslinks within a polymer network is not limited to restoring mechanical strength after damage or facilitating material reprocessing. Healing or reprocessing should also lead to restoration of other essential functional properties. For example, a dynamic polymer to be used as a solid electrolyte should also regain its conductivity on healing or reprocessing. Several examples of healable adhesives and sealants based on dynamic polymer networks have already been reported.¹²⁸⁻¹³⁰ Certain applications such as semiconductor manufacturing also require adhesives with the ability to debond on demand, through dynamic bond cleavage.¹³¹ The ability to control the surface wetting and optical properties of dynamic interpenetrating networks through multiple stimuli, has also been recently reported as an attractive approach to design smart surfaces.¹³² An interesting application of the solid-state siloxane bond exchange in polydimethylsiloxane networks, followed by pyrolysis, for producing ceramics with intricate submicron features has been recently demonstrated by Zhao, Xie, and coworkers.¹³³ With the rising use of 3D printing for manufacture of custom designed thermoset parts, vitrimers offer the environmentally friendly convenience of welding, repairing, reshaping, and reprocessing used 3D printed parts.¹³⁴ Sun and coworkers have recently reported the design of atomic oxygen-resistant coatings capable of autonomous healing, as potential heat shields for spacecrafts operating in low earth orbit environments.¹³⁵ Polymers can be designed to be good insulators or good conductors of electricity. Consequently, dynamic polymers are widely used as healable materials for energy harvesting and energy storage devices, including wearable electronics.^{136, 137}

Dynamic polymers have already transitioned from being merely a topic of academic interest to real-world products with novel features. For example, Mallinda Inc. has developed resins and highly stable resin impregnated fibre mats (pre-pregs) based on their patented imine-crosslinked vitrimer technology with a wide range of glass transition temperatures ($T_g \approx 20$ °C to 240 °C).¹³⁸ The highly stable, pre-cured thermoset prepreps can be rapidly compression moulded into composite parts (< 1 minute), enabling high throughput production of components that can be closed-loop recycled, and enable damage repair as a result of the dynamic imine junctions in the resulting networks. NEI Corporation offers a series of self-healing protective coatings capable of thermally assisted healing, owing to the patented biphasic thermoset/thermoplastic polymer matrix.¹³⁹ Similarly, Suprapolix BV offers self-healable polymers based on quadruple hydrogen bonding interactions for a variety of applications ranging from adhesives and coatings, to biomedical materials.¹⁴⁰ Additionally, a SciFinder search for patents with English as a language filter, for the term “self

healing polymer” returned 260 references, while that for the terms “vitrimer,” “dynamic polymer,” and “dynamic thermoset” returned a total of 40 references, indicating the steady increase in commercial interest in these materials (access date: 12 September 2019).

The dynamic B—O bonds within boronic esters and boroxines are capable of undergoing bond exchange *via* both associative, and dissociative pathways, depending on ambient temperature and humidity levels. While dynamic behaviour in response to more than one stimulus (heat, and moisture in case of B—O bonds) is an added advantage, the moisture induced malleability in the resulting networks can lead to unwanted creep even at normal service temperatures. New approaches to overcome this limitation are required to ensure material robustness, along with efficient healing/recycling. Development of room-temperature healable stiff polymer networks, is an ongoing challenge, irrespective of the dynamic chemistry employed. Most of the literature examples of intrinsic network healing at room temperature involve soft, elastomeric materials, with considerable chain mobility at low temperatures.^{27, 86} A rare combination of superior toughness and rapid healing behaviour at room temperature, was obtained by embedding rapidly exchangeable aromatic disulphide units within the hard but non-crystalline segments of a linear thermoplastic polyurethane. The hydrogen bonds between urethane links provided added stiffness to the polymers, resulting in a peak tensile strength of 6.8 MPa, and a toughness value of 26.9 MJ m⁻³. This example highlights the important roles played by the choice and positioning of dynamic bonds through innovative macromolecular engineering to balance the interplay of chain mobility, bond exchange, and material stiffness. An analogous challenge lies in the design of vitrimers that can be rapidly reprocessed using conventional techniques such as extrusion. However, the viscous flow of a vitrimer is limited by the rate of dynamic bond exchange, and reprocessing is conventionally performed using slow techniques like compression moulding. Du Prez, Winne, and coworkers¹⁴¹ recently demonstrated that the optimal amount of bond exchange catalyst, in combination with a macromolecular architecture that favours rapid bond exchange, results in vitrimers that undergo fast relaxation (and flow) at conventional extrusion temperatures (150 °C). This example reiterates the equal importance of bond dynamics, and macromolecular architecture in tuning static and dynamic properties. Ultimately, it is the fine balance between the choice of dynamic bonds and their synergy, exploited through innovative macromolecular engineering, which will drive future research efforts in this area to provide robust, and durable dynamic polymers.

Summary and outlook

While the research towards intrinsically self-healing and reprocessable bulk thermoset polymers has continued to make important strides in the past decade, the use of reversible B—O bonds for designing such materials has only been explored in the past 5 years. Nonetheless, the limited amount of research reported thus far highlights the great potential of dynamic B—O bonds as reversible crosslinks in bulk thermoset polymers from a circular economy¹⁴² perspective. Notably, the reversibility of the B—O bonds in boronic esters and boroxines can be accessed *via* both dissociative and associative pathways,

enabling the fine-tuning of material properties along with healing and reprocessing efficiency. Some of the research highlighted in this review has also demonstrated the amenability of reversible B—O bonds to designing polymers that undergo healing/re-moulding at room-temperature — a desirable trait, for several applications where the component cannot be withdrawn from service during healing. However, the rapid rate of bond exchange that allows reprocessability at room temperature typically leads to materials that creep under these same moderate conditions. Therefore, new strategies are required to approach the delicate balance between healability/reprocessability and creep resistance. The influence of Lewis basic neighbouring groups on the healing kinetics for polymers containing either boronic esters or boroxines has been already demonstrated, and warrants further research efforts. While the bulk hydrophobicity of polymers, or addition

of Lewis-basic additives, seems to afford improved hydrolytic stability to the reversible B—O bonds in healable polymer networks, further research is required to elucidate the underlying structure-property relationships that maximize the mechanical and dimensional stability of dynamic polymers under high humidity and perhaps even when submerged in water for extended durations. In fact, regardless of the type of reversible bonds involved, there exists a significant knowledge gap about the effect of polymer architecture on the mechanical properties and healing/reprocessing efficiency.³⁹ In many applications, the restoration of a secondary functionality along with mechanical properties is desirable at the end of the healing/re-moulding process.¹⁴³ Considering the multitude of applications that organoboron polymers can be used for, it is only a matter of time before healable organoboron polymers

Table 1 Summary of mechanical properties, healing, and reprocessing results of various bulk network polymers based on dynamic B—O bonds.

Dynamic bond	Mechanical Properties			Healing conditions	Healing efficiency (%)	Reprocessability	Reference
	Peak Stress (MPa)	% strain at break	Young's modulus (MPa)				
Boronic ester	4.5 [#]	60	NA	3 days at rt and 85% RH	>90	NA	⁸⁶
Boronic ester	1.6 [#]	80	NA	3–7 days at rt and 85% RH	55–95 [†]	yes; prolonged exposure to 85% RH	¹⁰⁰
Boronic ester	1.32 [#]	1000–1600 [†]	NA	wetting + 1 day at rt	60–70 [†]	no	¹⁰¹
Boronic ester	1.7–2.7 [†]	200–500 [†]	1.85–2.45 [†]	24h at 80 °C	>80	yes; hot pressing for 1 h under 10 MPa, at 160 °C	¹⁰²
Boronic ester + Zn ²⁺ —O coordination	14.63 [#]	475	4.45 [#]	24h at 80 °C	>90	yes; hot pressing for 1 h under 10 MPa, at 160 °C	¹⁰³
Boronic ester	25–50 [†]	400–1400 [†]	500 [#]	NA	NA	yes; extrusion or compression- or injection-moulding	⁸⁹
Boronic ester with B—N dative bonds	1.85	350	4.7	16h at 50 °C	>95	yes; hot pressing at 80 °C	¹¹¹
Boronic ester with B—N dative bonds	4.6	300	4.1	3–7 days at rt and 75% RH	>95	yes; hot pressing at 60 °C, or cold pressing at rt after exposure to moisture	¹¹²
Boroxine	9.64	10	182	wetting + 12h at 70 °C	>95	NA	¹¹⁹
N-coordinated boroxines + H-bonding	1.7–12.7	81–661	2.7–112	wetting + 6–18h at rt	87–99	yes; wetting with ethanol + cold pressing at 0.4 kPa for 24 h	¹²¹
Iminoboronate-derived boroxines	3.9	292	61	48 h at ambient humidity and rt	93	NA	¹²²
Iminoboronate-derived boroxines	11	3	551	12h at 70% RH, or overnight at 70 °C	~100	yes; hot pressing under 1 MPa for 10 min at 80 °C for	¹²³
Boroxines with B—N dative bonds	17.8	13.7	559	NA	NA	yes; hot pressing at 80 °C	⁹⁵
Boroxines with B—N dative bonds	23	23	330 [#]	wetting + 24h at 55 °C	>90	yes; hot pressing under 4 MPa for 15 min at 60 °C	⁹⁷

NA = not available; rt = room temperature; RH = relative humidity; [#]highest reported value; [†]range, over multiple samples

with such capability become a reality. It is very likely that the future designs of healable or reprocessable polymers will employ a combination of two or more reversible bonds (including B—O bonds) that complement one another towards optimizing material properties and efficient healing for sophisticated functions. Considering the susceptibility of the carbon–boron bond in boronic acid derivatives to oxidation,^{144, 145} a detailed assessment of the oxidative stability of the dynamic organoboron species in these polymers shall provide valuable cues for developing new organoboron compounds and monomers containing reversible covalent bonds with improved long-term stability. Finally, most of the research highlighted in this review utilizes specially designed organoboron monomers, polymers, or crosslinkers that are either expensive, or obtained through multistep synthetic protocols. Further research towards improving current synthetic protocols or inventing new ones to ensure ready availability of organoboron monomers and functional polymers¹⁴⁶ with a small price tag should facilitate the commercialization of boron based dynamic polymers as viable alternatives to contemporary commodity thermosets.

Conflicts of interest

There are no conflicts to declare

Acknowledgements

This research was supported under Australian Research Council's Industrial Transformation Research Hub funding scheme (project number IH140100018) (AS). APB, and AS thank Dr. Surya Subianto for his valuable inputs. This material is based upon work supported by the National Science Foundation (DMR-1904631) (BSS).

References

1. R. Geyer, J. R. Jambeck and K. L. Law, *Science Advances*, 2017, **3**, e1700782.
2. D. K. Schneiderman and M. A. Hillmyer, *Macromolecules*, 2017, **50**, 3733-3749.
3. C. K. Williams and M. A. Hillmyer, *Polymer Reviews*, 2008, **48**, 1-10.
4. J.-B. Zhu, E. M. Watson, J. Tang and E. Y. X. Chen, *Science*, 2018, **360**, 398.
5. S. Yu, R. Zhang, Q. Wu, T. Chen and P. Sun, *Advanced Materials*, 2013, **25**, 4912-4917.
6. S. Yang, J.-S. Chen, H. Körner, T. Breiner, C. K. Ober and M. D. Poliks, *Chemistry of Materials*, 1998, **10**, 1475-1482.
7. Y. Yang, X. Ding and M. W. Urban, *Progress in Polymer Science*, 2015, **49-50**, 34-59.
8. X. Zhang, M. Fevre, G. O. Jones and R. M. Waymouth, *Chemical Reviews*, 2018, **118**, 839-885.
9. J. M. García, *Chem*, 2016, **1**, 813-815.
10. B. J. Blaiszik, S. L. B. Kramer, S. C. Olugebefola, J. S. Moore, N. R. Sottos and S. R. White, *Annual Review of Materials Research*, 2010, **40**, 179-211.
11. D. Y. Wu, S. Meure and D. Solomon, *Progress in Polymer Science*, 2008, **33**, 479-522.
12. R. P. Sijbesma, F. H. Beijer, L. Brunsveld, B. J. B. Folmer, J. H. K. K. Hirschberg, R. F. M. Lange, J. K. L. Lowe and E. W. Meijer, *Science*, 1997, **278**, 1601.
13. Y. Yanagisawa, Y. Nan, K. Okuro and T. Aida, *Science*, 2018, **359**, 72.
14. P. Cordier, F. Tournilhac, C. Soulié-Ziakovic and L. Leibler, *Nature*, 2008, **451**, 977.
15. Y. Chen, A. M. Kushner, G. A. Williams and Z. Guan, *Nature Chemistry*, 2012, **4**, 467.
16. M. W. Urban, D. Davydovich, Y. Yang, T. Demir, Y. Zhang and L. Casabianca, *Science*, 2018, **362**, 220.
17. S. Burattini, H. M. Colquhoun, J. D. Fox, D. Friedmann, B. W. Greenland, P. J. F. Harris, W. Hayes, M. E. Mackay and S. J. Rowan, *Chemical Communications*, 2009, DOI: 10.1039/B910648K, 6717-6719.
18. M. Burnworth, L. Tang, J. R. Kumpfer, A. J. Duncan, F. L. Beyer, G. L. Fiore, S. J. Rowan and C. Weder, *Nature*, 2011, **472**, 334.
19. R. J. Varley and S. van der Zwaag, *Acta Materialia*, 2008, **56**, 5737-5750.
20. Y.-F. Wang, D.-L. Zhang, T. Zhou, H.-S. Zhang, W.-Z. Zhang, L. Luo, A.-M. Zhang, B.-J. Li and S. Zhang, *Polymer Chemistry*, 2014, **5**, 2922-2927.
21. S. J. Rowan, S. J. Cantrill, G. R. L. Cousins, J. K. M. Sanders and J. F. Stoddart, *Angewandte Chemie International Edition*, 2002, **41**, 898-952.
22. J.-M. Lehn, *Chemistry – A European Journal*, 1999, **5**, 2455-2463.
23. R. J. Wojtecki, M. A. Meador and S. J. Rowan, *Nature Materials*, 2010, **10**, 14.
24. X. Chen, M. A. Dam, K. Ono, A. Mal, H. Shen, S. R. Nutt, K. Sheran and F. Wudl, *Science*, 2002, **295**, 1698.
25. C.-M. Chung, Y.-S. Roh, S.-Y. Cho and J.-G. Kim, *Chemistry of Materials*, 2004, **16**, 3982-3984.
26. M. Pepels, I. Filot, B. Klumperman and H. Goossens, *Polymer Chemistry*, 2013, **4**, 4955-4965.
27. A. Rekondo, R. Martin, A. Ruiz de Luzuriaga, G. Cabañero, H. J. Grande and I. Odriozola, *Materials Horizons*, 2014, **1**, 237-240.
28. B. Zhang, Z. A. Digby, J. A. Flum, P. Chakma, J. M. Saul, J. L. Sparks and D. Konkolewicz, *Macromolecules*, 2016, **49**, 6871-6878.
29. Z. P. Zhang, M. Z. Rong, M. Q. Zhang and C. e. Yuan, *Polymer Chemistry*, 2013, **4**, 4648-4654.
30. Y. Amamoto, H. Otsuka, A. Takahara and K. Matyjaszewski, *Advanced Materials*, 2012, **24**, 3975-3980.
31. Z. P. Zhang, M. Z. Rong and M. Q. Zhang, *Advanced Functional Materials*, 2018, **28**, 1706050.
32. K. Imato, A. Takahara and H. Otsuka, *Macromolecules*, 2015, **48**, 5632-5639.
33. Y.-X. Lu and Z. Guan, *Journal of the American Chemical Society*, 2012, **134**, 14226-14231.
34. M. Capelot, D. Montarnal, F. Tournilhac and L. Leibler, *Journal of the American Chemical Society*, 2012, **134**, 7664-7667.
35. M. D. Hager, S. van der Zwaag and U. S. Schubert, eds., *Self-healing Materials*, Springer, Cham, Switzerland, 2016.

36. E. Tsangouri, D. Aggelis and D. Van Hemelrijck, *Progress in Polymer Science*, 2015, **49-50**, 154-174.
37. X. K. D. Hillewaere and F. E. Du Prez, *Progress in Polymer Science*, 2015, **49-50**, 121-153.
38. G. O. Wilson, H. M. Andersson, S. R. White, N. R. Sottos, J. S. Moore and P. V. Braun, *Self-Healing Polymers*, 2010.
39. S. J. Garcia, *European Polymer Journal*, 2014, **53**, 118-125.
40. D. Döhler, P. Michael and W. Binder, *Principles of Self-Healing Polymers*, 2013.
41. Y. Yang and M. W. Urban, in *Healable Polymer Systems*, The Royal Society of Chemistry, 2013, DOI: 10.1039/9781849737470-00126, pp. 126-148.
42. Y. Yang and M. W. Urban, *Chemical Society Reviews*, 2013, **42**, 7446-7467.
43. S. R. White, M. M. Caruso and J. S. Moore, *MRS Bulletin*, 2008, **33**, 766-769.
44. B. A. Helms and T. P. Russell, *Chem*, 2016, **1**, 816-818.
45. D. J. Fortman, J. P. Brutman, G. X. De Hoe, R. L. Snyder, W. R. Dichtel and M. A. Hillmyer, *ACS Sustainable Chemistry & Engineering*, 2018, **6**, 11145-11159.
46. W. Denissen, J. M. Winne and F. E. Du Prez, *Chemical Science*, 2016, **7**, 30-38.
47. C. J. Kloxin and C. N. Bowman, *Chemical Society Reviews*, 2013, **42**, 7161-7173.
48. C. J. Kloxin, T. F. Scott, B. J. Adzima and C. N. Bowman, *Macromolecules*, 2010, **43**, 2643-2653.
49. D. Montarnal, M. Capelot, F. Tournilhac and L. Leibler, *Science*, 2011, **334**, 965.
50. M. Capelot, M. M. Unterlass, F. Tournilhac and L. Leibler, *ACS Macro Letters*, 2012, **1**, 789-792.
51. W. Denissen, G. Rivero, R. Nicolaÿ, L. Leibler, J. M. Winne and F. E. Du Prez, *Advanced Functional Materials*, 2015, **25**, 2451-2457.
52. M. M. Obadia, B. P. Mudraboyina, A. Serghei, D. Montarnal and E. Drockenmuller, *Journal of the American Chemical Society*, 2015, **137**, 6078-6083.
53. P. Zheng and T. J. McCarthy, *Journal of the American Chemical Society*, 2012, **134**, 2024-2027.
54. Y.-X. Lu, F. Tournilhac, L. Leibler and Z. Guan, *Journal of the American Chemical Society*, 2012, **134**, 8424-8427.
55. P. Taynton, K. Yu, R. K. Shoemaker, Y. Jin, H. J. Qi and W. Zhang, *Advanced Materials*, 2014, **26**, 3938-3942.
56. P. R. Christensen, A. M. Scheuermann, K. E. Loeffler and B. A. Helms, *Nature Chemistry*, 2019, **11**, 442-448.
57. J. J. Lessard, L. F. Garcia, C. P. Easterling, M. B. Sims, K. C. Bentz, S. Arencibia, D. A. Savin and B. S. Sumerlin, *Macromolecules*, 2019, **52**, 2105-2111.
58. F. Jäkle, *Coordination Chemistry Reviews*, 2006, **250**, 1107-1121.
59. K. Tanaka and Y. Chujo, *Macromolecular Rapid Communications*, 2012, **33**, 1235-1255.
60. C. D. Entwistle and T. B. Marder, *Angewandte Chemie International Edition*, 2002, **41**, 2927-2931.
61. C. D. Entwistle and T. B. Marder, *Chemistry of Materials*, 2004, **16**, 4574-4585.
62. P. Puneet, R. Vedarajan and N. Matsumi, *ACS Sensors*, 2016, **1**, 1198-1202.
63. B. M. Squeo, V. G. Gregoriou, A. Avgeropoulos, S. Baysec, S. Allard, U. Scherf and C. L. Chochos, *Progress in Polymer Science*, 2017, **71**, 26-52.
64. F. Cheng, E. M. Bonder and F. Jäkle, *Journal of the American Chemical Society*, 2013, **135**, 17286-17289.
65. J. Shim, J. S. Lee, J. H. Lee, H. J. Kim and J.-C. Lee, *ACS Applied Materials & Interfaces*, 2016, **8**, 27740-27752.
66. A. B. Morgan, J. L. Jurs and J. M. Tour, *Journal of Applied Polymer Science*, 2000, **76**, 1257-1268.
67. Y. Zhang, T. Cai, W. Shang, L. Sun, D. Liu, D. Tong and S. Liu, *Tribology International*, 2017, **115**, 297-306.
68. A. Ledoux, P. Larini, C. Boisson, V. Monteil, J. Raynaud and E. Lacôte, *Angewandte Chemie*, 2015, **127**, 15970-15975.
69. W. L. A. Brooks and B. S. Sumerlin, *Chemical Reviews*, 2016, **116**, 1375-1397.
70. J. N. Cambre and B. S. Sumerlin, *Polymer*, 2011, **52**, 4631-4643.
71. F. Vidal, H. Lin, C. Morales and F. Jäkle, *Molecules*, 2018, **23**.
72. D. Roy, J. N. Cambre and B. S. Sumerlin, *Chemical Communications*, 2008, DOI: 10.1039/B802293C, 2477-2479.
73. C. C. Deng, W. L. A. Brooks, K. A. Abboud and B. S. Sumerlin, *ACS Macro Letters*, 2015, **4**, 220-224.
74. K. T. Kim, J. J. L. M. Cornelissen, R. J. M. Nolte and J. C. M. v. Hest, *Journal of the American Chemical Society*, 2009, **131**, 13908-13909.
75. F. Kuralay, S. Sattayasamitsathit, W. Gao, A. Uygun, A. Katzenberg and J. Wang, *Journal of the American Chemical Society*, 2012, **134**, 15217-15220.
76. R. Ma and L. Shi, *Polymer Chemistry*, 2014, **5**, 1503-1518.
77. J. Xu, D. Yang, W. Li, Y. Gao, H. Chen and H. Li, *Polymer*, 2011, **52**, 4268-4276.
78. V. Yesilyurt, M. J. Webber, E. A. Appel, C. Godwin, R. Langer and D. G. Anderson, *Advanced Materials*, 2016, **28**, 86-91.
79. M. C. Roberts, M. C. Hanson, A. P. Massey, E. A. Karren and P. F. Kiser, *Advanced Materials*, 2007, **19**, 2503-2507.
80. S. Tang, H. Ma, H.-C. Tu, H.-R. Wang, P.-C. Lin and K. S. Anseth, *Advanced Science*, 2018, **5**, 1800638.
81. A. Mahalingam, A. R. Geonnotti, J. Balzarini and P. F. Kiser, *Molecular Pharmaceutics*, 2011, **8**, 2465-2475.
82. Y. Kotsuchibashi, R. V. C. Agustin, J.-Y. Lu, D. G. Hall and R. Narain, *ACS Macro Letters*, 2013, **2**, 260-264.
83. Y. Chen, D. Diaz-Dussan, D. Wu, W. Wang, Y.-Y. Peng, A. B. Asha, D. G. Hall, K. Ishihara and R. Narain, *ACS Macro Letters*, 2018, **7**, 904-908.
84. Y. Guan and Y. Zhang, *Chemical Society Reviews*, 2013, **42**, 8106-8121.
85. B. Marco-Dufort and M. W. Tibbitt, *Materials Today Chemistry*, 2019, **12**, 16-33.
86. J. J. Cash, T. Kubo, A. P. Bapat and B. S. Sumerlin, *Macromolecules*, 2015, **48**, 2098-2106.
87. W. Niu, C. O'Sullivan, B. M. Rambo, M. D. Smith and J. J. Lavigne, *Chemical Communications*, 2005, DOI: 10.1039/B504634C, 4342-4344.
88. A. P. Bapat, D. Roy, J. G. Ray, D. A. Savin and B. S. Sumerlin, *Journal of the American Chemical Society*, 2011, **133**, 19832-19838.
89. M. Röttger, T. Domenech, R. van der Weegen, A. Breuillac, R. Nicolaÿ and L. Leibler, *Science*, 2017, **356**, 62.
90. A. L. Korich and P. M. Iovine, *Dalton Transactions*, 2010, **39**, 1423-1431.
91. P. De, S. R. Gondi, D. Roy and B. S. Sumerlin, *Macromolecules*, 2009, **42**, 5614-5621.
92. Y. Qin, C. Cui and F. Jäkle, *Macromolecules*, 2007, **40**, 1413-1420.

93. A. P. Côté, A. I. Benin, N. W. Ockwig, M. Keeffe, A. J. Matzger and O. M. Yaghi, *Science*, 2005, **310**, 1166.
94. Y. Tokunaga, H. Ueno and Y. Shimomura, *Heterocycles*, 2007, **74**, 219-223.
95. W. A. Ogden and Z. Guan, *Journal of the American Chemical Society*, 2018, **140**, 6217-6220.
96. P. M. Iovine, C. R. Gyselbrecht, E. K. Perttu, C. Klick, A. Neuwelt, J. Loera, A. G. DiPasquale, A. L. Rheingold and J. Kua, *Dalton Transactions*, 2008, DOI: 10.1039/B804705G, 3791-3794.
97. C. Bao, Z. Guo, H. Sun and J. Sun, *ACS Applied Materials & Interfaces*, 2019, **11**, 9478-9486.
98. E. B. Stukalin, L.-H. Cai, N. A. Kumar, L. Leibler and M. Rubinstein, *Macromolecules*, 2013, **46**, 7525-7541.
99. L. Li, X. Chen, K. Jin and J. M. Torkelson, *Macromolecules*, 2018, **51**, 5537-5546.
100. J. J. Cash, T. Kubo, D. J. Dobbins and B. S. Sumerlin, *Polymer Chemistry*, 2018, **9**, 2011-2020.
101. Y. Zuo, Z. Gou, C. Zhang and S. Feng, *Macromolecular Rapid Communications*, 2016, **37**, 1052-1059.
102. Y. Chen, Z. Tang, X. Zhang, Y. Liu, S. Wu and B. Guo, *ACS Applied Materials & Interfaces*, 2018, **10**, 24224-24231.
103. Y. Chen, Z. Tang, Y. Liu, S. Wu and B. Guo, *Macromolecules*, 2019, DOI: 10.1021/acs.macromol.9b00419.
104. W. C. Yount, D. M. Loveless and S. L. Craig, *Journal of the American Chemical Society*, 2005, **127**, 14488-14496.
105. W. Weng, J. B. Beck, A. M. Jamieson and S. J. Rowan, *Journal of the American Chemical Society*, 2006, **128**, 11663-11672.
106. H. Ying, Y. Zhang and J. Cheng, *Nature Communications*, 2014, **5**, 3218.
107. J. Brassinne, J.-F. Gohy and C.-A. Fustin, *ACS Macro Letters*, 2016, **5**, 1364-1368.
108. G. Wulff, M. Lauer and H. Böhnke, *Angewandte Chemie International Edition in English*, 1984, **23**, 741-742.
109. L. Zhu, S. H. Shabbir, M. Gray, V. M. Lynch, S. Sorey and E. V. Anslyn, *Journal of the American Chemical Society*, 2006, **128**, 1222-1232.
110. H. Li, Y. Liu, J. Liu and Z. Liu, *Chemical Communications*, 2011, **47**, 8169-8171.
111. O. R. Cromwell, J. Chung and Z. Guan, *Journal of the American Chemical Society*, 2015, **137**, 6492-6495.
112. C. Kim, H. Ejima and N. Yoshie, *Journal of Materials Chemistry A*, 2018, **6**, 19643-19652.
113. C. Kim, H. Ejima and N. Yoshie, *RSC Advances*, 2017, **7**, 19288-19295.
114. S. Wang, X. Xing, X. Zhang, X. Wang and X. Jing, *Journal of Materials Chemistry A*, 2018, **6**, 10868-10878.
115. E. Sheepwash, V. Krampfl, R. Scopelliti, O. Sereda, A. Neels and K. Severin, *Angewandte Chemie International Edition*, 2011, **50**, 3034-3037.
116. J. Cruz-Huerta, D. Salazar-Mendoza, J. Hernández-Paredes, I. F. Hernández Ahuactzi and H. Höpfl, *Chemical Communications*, 2012, **48**, 4241-4243.
117. N. Luisier, R. Scopelliti and K. Severin, *Soft Matter*, 2016, **12**, 588-593.
118. S. Ito, H. Takata, K. Ono and N. Iwasawa, *Angewandte Chemie*, 2013, **125**, 11251-11254.
119. J.-C. Lai, J.-F. Mei, X.-Y. Jia, C.-H. Li, X.-Z. You and Z. Bao, *Advanced Materials*, 2016, **28**, 8277-8282.
120. J. Kua and P. M. Iovine, *The Journal of Physical Chemistry A*, 2005, **109**, 8938-8943.
121. C. Bao, Y.-J. Jiang, H. Zhang, X. Lu and J. Sun, *Advanced Functional Materials*, 2018, **28**, 1800560.
122. S. Delpierre, B. Willocq, J. De Winter, P. Dubois, P. Gerbaux and J.-M. Raquez, *Chemistry – A European Journal*, 2017, **23**, 6730-6735.
123. S. Delpierre, B. Willocq, G. Manini, V. Lemaure, J. Goole, P. Gerbaux, J. Cornil, P. Dubois and J.-M. Raquez, *Chemistry of Materials*, 2019, DOI: 10.1021/acs.chemmater.9b00750.
124. Q. Guo, B. Huang, C. Lu, T. Zhou, G. Su, L. Jia and X. Zhang, *Materials Horizons*, 2019, **6**, 996-1004.
125. G. M. Scheutz, J. J. Lessard, M. B. Sims and B. S. Sumerlin, *Journal of the American Chemical Society*, 2019, DOI: 10.1021/jacs.9b07922.
126. T.-P. Huynh, P. Sonar and H. Haick, *Advanced Materials*, 2017, **29**, 1604973.
127. P. Taynton, H. Ni, C. Zhu, K. Yu, S. Loob, Y. Jin, H. J. Qi and W. Zhang, *Advanced Materials*, 2016, **28**, 2904-2909.
128. D.-P. Wang, Z.-H. Zhao, C.-H. Li and J.-L. Zuo, *Materials Chemistry Frontiers*, 2019, **3**, 1411-1421.
129. S. Wang, Z. Liu, L. Zhang, Y. Guo, J. Song, J. Lou, Q. Guan, C. He and Z. You, *Materials Chemistry Frontiers*, 2019, **3**, 1833-1839.
130. W. Gao, M. Bie, F. Liu, P. Chang and Y. Quan, *ACS Applied Materials & Interfaces*, 2017, **9**, 15798-15808.
131. D. K. Hohl and C. Weder, *Advanced Optical Materials*, 2019, **7**, 1900230.
132. L. Zhou, T. Ma, T. Li, X. Ma, J. Yin and X. Jiang, *ACS Applied Materials & Interfaces*, 2019, **11**, 15977-15985.
133. N. Zheng, J. Hou, H. Zhao, J. Wu, Y. Luo, H. Bai, J. A. Rogers, Q. Zhao and T. Xie, *Advanced Materials*, 2019, **31**, 1807326.
134. B. Zhang, K. Kowsari, A. Serjouei, M. L. Dunn and Q. Ge, *Nature Communications*, 2018, **9**, 1831.
135. X. Wang, Y. Li, Y. Qian, H. Qi, J. Li and J. Sun, *Advanced Materials*, 2018, **30**, 1803854.
136. D. Chen, D. Wang, Y. Yang, Q. Huang, S. Zhu and Z. Zheng, *Advanced Energy Materials*, 2017, **7**, 1700890.
137. J. Deng, X. Kuang, R. Liu, W. Ding, A. C. Wang, Y.-C. Lai, K. Dong, Z. Wen, Y. Wang, L. Wang, H. J. Qi, T. Zhang and Z. L. Wang, *Advanced Materials*, 2018, **30**, 1705918.
138. Mallinda Inc. , <https://www.mallinda.com>, (accessed 13 September 2019).
139. NEI Corporation. Advanced protective coatings: self-healing., <https://www.neicorporation.com/products/coatings/self-healing-coatings/>, (accessed 13 September 2019).
140. Suprapolix BV, <http://www.suprapolix.com/pages/polymers>, (accessed 13 September 2019).
141. C. Taplan, M. Guerre, J. M. Winne and F. E. Du Prez, *Materials Horizons*, 2019, DOI: 10.1039/C9MH01062A.
142. Circular Economy: Concept, <https://www.ellenmacarthurfoundation.org/circular-economy/concept>, (accessed 31 July 2019).
143. J. Ahner, S. Bode, M. Micheel, B. Dietzek and M. D. Hager, in *Self-healing Materials*, eds. M. D. Hager, S. van der Zwaag and U. S. Schubert, Springer International Publishing, Cham, 2016, DOI: 10.1007/12_2015_333, pp. 247-283.
144. K. S. Webb and D. Levy, *Tetrahedron Letters*, 1995, **36**, 5117-5118.
145. Y. Cui, M. Zhang, F.-S. Du and Z.-C. Li, *ACS Macro Letters*, 2017, **6**, 11-15.

ARTICLE

Journal Name

146. T. Kubo, G. M. Scheutz, T. S. Latty and B. S. Sumerlin, *Chemical Communications*, 2019, **55**, 5655-5658.